Interplay of opposing fate choices stalls oncogenic growth in skin epithelium

Madeline V Sandoval

A dissertation

submitted in partial fulfillment of the

requirement for the degree of

Doctor of Philosophy

University of Washington

2020

Reading Committee:

Slobodan Beronja, Chair

Valeri Vasioukhin

Cyrus Ghajar

Program authorized to Offer Degree:

Molecular and Cellular Biology

University of Washington

Abstract

Interplay of opposing fate choices stalls oncogenic growth in skin epithelium

Madeline V Sandoval

Chair of the Supervisory Committee:

Slobodan Beronja

Division of Human Biology, Fred Hutchinson Cancer Research Center

Due to its exposed nature, skin is subject to continuous DNA damage and a high incidence of oncogenic mutations. To ensure normal function it repairs or expels damaged cells. However, the skin is also able to tolerate numerous long-lived oncogenic clones that can comprise a significant portion of physiologically normal adult tissue, but how it does so is unknown. In highly mutagenized skin, it is thought that oncogenic clones can compete with each other and stall one another's growth to maintain tissue structure and function. But how such tolerance is established in the context of early, independently occurring single oncogenic events remains undiscovered. To directly address this question, we induce $Hras^{G12V}$ expression in single cells in the adult murine epidermis and follow them long-term. Using a novel cell fate identification (CFI) assay that can directly quantify progenitor cell fate choice *in vivo*, we show that $Hras^{G12V}$ induces an early and transient pro-growth effect driven by increased progenitor renewal. Ultimately, renewal yields to progenitor differentiation, leading to stalled clone expansion. CFI allowed us to attribute this

dynamic effect on the emergence of two distinct populations within oncogenic clones, renewing progenitors along the edge and differentiating ones within the central core. As clone expansion is accompanied by progressive enlargement of the core and diminishment of the edge compartment, the interplay between the two populations works to stabilize oncogenic growth. In order to identify the molecular pathway that governs $Hras^{G12V}$-driven differentiation, we employ an shRNA-mediated screen of Ras-effectors *in vivo*. The screen identifies Rassf5 as the top candidate, which we further validate as a novel mediator that is both necessary and sufficient for oncogene-specific progenitor differentiation. Our study provides evidence that the epidermis can tolerate an isolated oncogenic event through a novel cellular mechanism of inter-clonal competition.

Acknowledgements

My personal journey to a doctorate has been a long, winding road but not without guidance and support along the way. First, I would like to thank Boba for being an enthusiastic and patient advisor.

Thank you to all the members of the Beronja Lab—Paula, Julie, Kamya, Zhe, Elise, Na, Megan, Maddie, and Wei. I felt that we always had a very positive lab environment, which made work enjoyable. I would like to give a special thank you to Zhe, who was always incredibly helpful and knowledgeable about all things science.

I would also like to thank my committee members Cecilia, Hannele, Valera, and Cyrus for pushing me to develop as a scientist.

Thank you to my siblings and friends for their constant support. And to my fellow grad students Elise, Eli, George, and Kristine, thank you for the solidarity. Many thanks to my parents for instilling within me a love of learning, hard work and resilience, and also to my in-laws for their indomitable positivity.

And finally, thanks to Tim. Without you, I couldn't have done it.

Table of Contents

List of Figures

Chapter 1—Introduction

1.1 Cell competition

Tissues are composed of an array of unique cell types. Individual cells, even those that are homotypic, are non-identical, with differences in mitotic capabilities, signaling sensitivity, location, etc. Cells have the ability to sense the fitness levels of their neighbors. This creates a competition between cells that are intrinsically more fit than their counterparts, which ultimately results in the removal of less fit but still viable cells. This elimination can be in the form of extrusion, differentiation, senescence, phagocytosis or apoptosis. After the removal of the less fit cell, the tissue compensates for its loss by hypertrophy or increased proliferation (Bowling et al., 2019), making cell competition a phenotypically silent process (Figure 1).

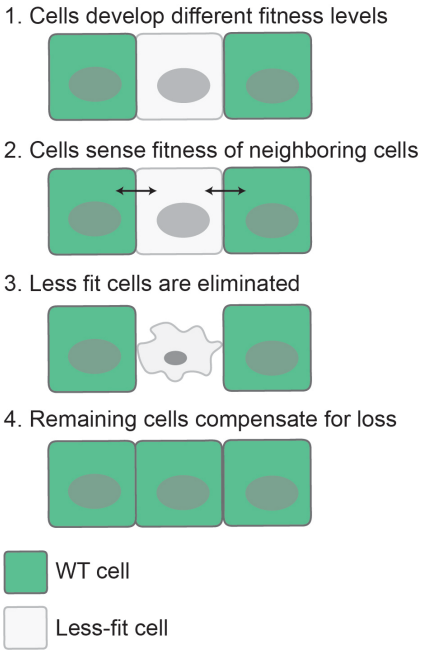

Figure 1: Cell competition induces the removal of cells with lower fitness

This phenomenon was first observed in *Drosophila* Minute mutants. Homozygous Minute mutations are lethal but heterozygous Minute mutations are viable, though the animals develop more slowly. When less-fit Minute$^{+/-}$ clones were initiated on a wild-type (WT) background, they were removed from the tissue via apoptosis triggered by the surrounding WT cells (Morata and Ripoll, 1975). Further study discovered that cells containing mutations in ribosome gene Rpl24 were outcompeted in developing mouse embryos (Oliver et al., 2004), effectively expanding the cell competition field into mammalian tissues. Cell competition has also been implicated in organ development. If Myc is overexpressed in all cells in a developing *Drosophila* wing, the entire wing increases in size. However, if Myc expression varies throughout the developing tissue, low-Myc expressing cells

will undergo apoptosis and high-Myc cells will compensate, resulting in the formation of a normal sized wing (de la Cova et al., 2004).

Deleterious mutations are not the sole method of altering a cell's fitness. Myc is an example of this. A beneficial mutation would make the mutant cell able to out compete WT cells, rendering the mutant population "super fit" (Bowling et al., 2019). This is seen in the clonal expansion of mouse epidermal cells driven by mutant *Trp53* (Murai et al., 2018), and in the ability of *dMyc* overexpressing cells to eliminate their WT neighbors and easily colonize *Drosophila* epithelium (Moreno and Basler, 2004). Tissues have evolved mechanisms to identify and remove high fitness cells. Mechanical stress-induced competition leads to the extrusion of live cells in human colon, zebrafish and cultured Madin-Darby canine kidney (MDCK) cells (Eisenhoffer et al., 2012). This observation suggests that cell extrusion, in the context of hyperproliferation of cells, can act as a tumor suppression mechanism by correcting the over expansion of a mass of cells and returning the epithelium to homeostasis. Additional work established that MDCK cells can identify a Ras^{V12} expressing cell and remove it from the epithelial sheet (Hogan et al., 2009), providing evidence of a mechanism which enables WT cells to sense oncogene-expressing cells. This further establishes cell competition as a method of hindering tumor growth.

However, cell competition can fail at eliminating cells with aberrant mitogenic potential. Recent deep sequencing experiments discovered that physiologically normal, but aged, sun-exposed skin contained numerous, diverse mutations. Of the cells sequenced, 25-50% contained a lesion in a gene considered important for driving squamous cell carcinoma. A striking feature of this surprising tolerance is mutant clones that persist in the tissue are both limited and uniform in size, irrespective of a mutation's proliferative ability (Martincorena et al., 2015). One explanation for this observation is a model of inter-clone growth inhibition wherein the super fit mutant clones

compete with each other, thereby suppressing growth. (Bowling et al., 2019; Higa and DeGregori, 2019). This idea has been modeled in murine epidermis. Gain of function mutant p53 clones expand extensively in naïve epidermis. However, p53 clones do not grow as extensively in UV exposed epidermis, implying that UV-induced mutations rendered the WT basal cells more able to compete and thus impede p53 clone expansion (Murai et al., 2018).

The presence of numerous, oncogenic clones burdening a normal tissue was again observed in the esophagus (Martincorena et al., 2018). Remarkably, the average number of mutations per cell in the esophagus is about 1/10 that of sun-exposed skin, but there is a higher density of cancer-causing mutations in esophagus compared to sun exposed skin. NOTCH1 was more frequently mutated in normal esophagus than is seen in esophageal squamous cell carcinoma, leading the authors to conclude that mutations which impede transformation may be beneficial to the tissue.

The multiclonal model of tumor-suppression and the idea of specific mutations, like NOTCH1, preventing further transformation provide a model of how clone overgrowth can be controlled via cell competition. What is lacking is a mechanism to explain how the growth of a single clone can be constrained, an event that would occur many times in an exposed tissue such as the skin. The purpose of this study is to understand how a tissue can tolerate individual oncogenic clones. In order to investigate this question, we turn to the epidermis, a highly structured and experimentally tractable tissue, to observe the interplay between WT and oncogene-expressing cells.

1.2 Structure of the epidermis

Skin separates an organism from its external environment, functioning as a barrier to pathogens, UV-damage, physical trauma, dehydration, and temperature fluctuations. This organ is composed of two layers, the dermis and the epidermis (Figure 2). The dermis consists of muscle,

fat, nerves, blood vessels, and fibroblasts. The epidermis is comprised of epithelial cells organized in a proliferative basal layer and several stratified layers of differentiated cells. These layers (stratum spinosum and stratum granulosum), though non-dividing are transcriptionally active and express unique markers such as keratin 10 (K10) and Involucrin. The cells of the outer most layer of the skin (stratum corneum) express the terminal differentiation maker Filaggrin and are dead. Interspersed in the interfollicular epidermis (IFE) are numerous hair follicles. Though keratinocytes make up both the IFE and hair follicles, these two regions are still structurally and physiologically distinct (Gonzales and Fuchs, 2017).

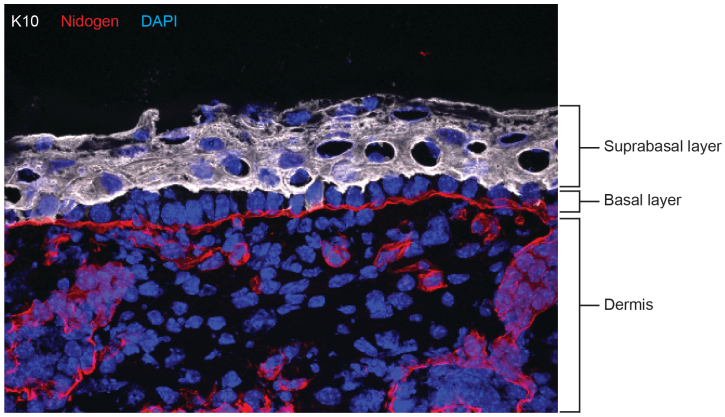

Figure 2 The basement membrane separates the epidermis from the dermis. The epidermis is composed of two populations: the basal cells (proliferative) and the suprabasal cells (non-proliferative).

The hair follicle has been extensively studied as a prime example of stem cell activity. Hair follicle stem cells reside in the bulge, a region located in the upper segment of the follicle (Myung and Ito, 2012). These stem cells are relatively quiescent (Sotiropoulou and Blanpain, 2012) and multipotent—giving rise to all epidermal lineages (Oshima et al., 2001; Rochat et al., 1994). The hair follicle undergoes complete restructuring as it moves through the phases of the hair cycle. After a period of quiescence (telogen), cells in the hair germ are activated along with bulge stem cells and begin to proliferate and extend the hair follicle (Levy et al., 2005; Morris et al., 2004; Rompolas et al., 2012). This growth phase (anagen) is followed by differentiation wherein the bulge stem cells primarily contribute to the formation of the outer root sheath. The cells of the inner root sheath continue to proliferate and differentiate, eventually forming the hair shaft. Following this growth phase, hair follicle cells undergo apoptosis, leading to the regression of the

structure (catagen) (Lindner et al., 1997). The follicle then enters telogen, and cell activity stops until the next cycle.

In contrast to relying on long lived quiescent cells to maintain progenitor identity, the IFE is composed of progenitor cells, though there is debate over their organization, maintenance, and cellular potency. It is known that progenitors give rise to the differentiated keratinocytes lying superior to the basal layer, and this process of progenitor renewal and differentiation is tightly controlled in order to maintain the integrity of the epidermis. Numerous studies propose that IFE progenitor cells are equipotent, dividing and differentiating stochastically (Clayton et al., 2007; Doupe et al., 2010). Live imaging of progenitor cell division and differentiation suggests that progenitor division is initiated based on delamination of nearby cells. Overall, the link between cell fate and cell division is balanced in order to maintain epidermis homeostasis. (Mesa et al., 2018; Rompolas et al., 2016). This allows the IFE to be self-sustaining but if wounded, HF stem cells can contribute to repopulation, but do not persist in the region and are eventually removed (Ito et al., 2005; Tumbar et al., 2004).

Conversely, there is also evidence of a stem cell hierarchy in the IFE. When using genetic lineage tracing via a K14 promoter and an Involucrin promoter, two distinct classes of stem cells were revealed: slow-cycling stem cells and committed progenitor cells. It appears that the slow-cycling stem cells give rise to committed progenitor cells and specifically express markers associated with IFE progenitor cells such as $\alpha 6$ and $\beta 1$ integrins. Furthermore, the slow-cycling and committed progenitor populations contribute to wound healing in different manners (Mascre et al., 2012; Sada et al., 2016). These findings bring the notion of equipotent epidermal progenitor cells into question, thus further study is needed to resolve the hierarchical identities of IFE progenitor cells.

1.3 Molecular mechanisms of progenitor cell maintenance

Perhaps the key feature of stem cells is the ability to maintain a pool of undifferentiated cells while also giving rise to differentiated progeny. In the epidermis, all basal cells express p63 whereas differentiated cells do not express p63. (Yang et al., 1998). p63 knockout animals do not completely form various squamous epitheliums including the esophagus, part of the stomach, and the skin. Specifically, the epidermis of p63 knockout animals is undeveloped and lacks skin derived appendages such as hair follicles, sebaceous glands, and mammary glands, delineating the significance of this gene in epithelial development. Moreover, epidermis that lacks p63 expression does not initiate keratin 5 (K5) expression during development, implying that p63 is relevant to basal cell identity. (Parsa et al., 1999; Yang et al., 1999). Another component of progenitor identity is expression of adhesion molecules. Basal cells attach to the basement membrane via integrins $\alpha6\beta4$ and $\alpha3\beta1$ (Watt and Jones, 1993). Cross-linking integrins inhibited differentiation of cultured keratinocytes (Adams and Watt, 1989). Integrin $\beta4$ also contributes to basal cell proliferation (Nikolopoulos et al., 2005). These individual components work together to ensure progenitor maintenance and proper function.

In order to produce differentiated daughter cells, progenitor cells often undergo asymmetric divisions, with one daughter remaining a progenitor and the other inheriting asymmetrically localized cell contents, creating a daughter cell which has a nonidentical renewal/differentiation potential. In *Drosophila* neuroblasts, the mechanism of asymmetric division is direct. These neural stem cells are structured with an apical and a basal side, and the orientation of the mitotic spindle determines the fate of the two daughter cells. This intrinsic polarization assists in apically localizing specific proteins such as Par-3, Par-6, and aPKC (Goldstein and Macara, 2007; Suzuki and Ohno, 2006). These factors orient the mitotic spindle and help to segregate fate determinants

like Numb. Numb inhibits differentiation by repressing the Notch pathway (Le Borgne et al., 2005; Schweisguth, 2004). In *Drosophila* neuroblasts, if a daughter cell inherits Numb, renewal processes are suppressed, and the cell differentiates into a ganglion mother cell.

An alternate method of generating asymmetric fates is to position cell division so that only one daughter cell retains a connection with the stem cell niche, thus maintaining the ability to renew. The *Drosophila* ovary stem cell niche contains 2-3 germline stem cells that are surrounded by cap cells. These cap cells secrete BMP ligands (Gpp and Dpp), which cause the transcriptional repression of Bam. When a daughter cell leaves the niche, it begins to express Bam, which in turn antagonizes stem cell renewal pathways and differentiation commences. The formation of a niche to control stem cell fate can provide a degree of maneuverability in stem cell identity and is more often found in adult animals (Knoblich, 2008).

Asymmetric division is a vital mechanism during development because it is the method that basal cells use to stratify the epithelium beginning at embryonic day 13.5 (E13.5) (Lechler and Fuchs, 2007). Some of the events that coordinate oriented divisions in *Drosophila* are conserved in the mouse. In murine epidermis, asymmetric cell division machinery localizes to the apical side of the cell. Apical/basal polarity is determined by Par3 interaction with the mInsc/Pins complex. mInsc/Pins recruits $G\alpha_{i3}$, which then complexes with LGN (Williams et al., 2014). LGN and NuMA interact to direct the orientation of the mitotic spindle in embryonic epidermis (Williams et al., 2011). When LGN is knocked down, keratinocytes preferentially undergo symmetric divisions and stratification of the epidermis is inhibited, however, cell polarity is maintained. Loss of LGN inhibits Notch activity, implying that asymmetric cell division and Notch work in a unified pathway to promote epidermal differentiation (Williams et al., 2011). A definitive, asymmetrically inherited cell fate driver has yet to be discovered in keratinocytes,

though Numb has been shown to be asymmetrically partitioned between daughter cells (Clayton et al., 2007), pointing to the importance of Notch signaling in keratinocyte differentiation.

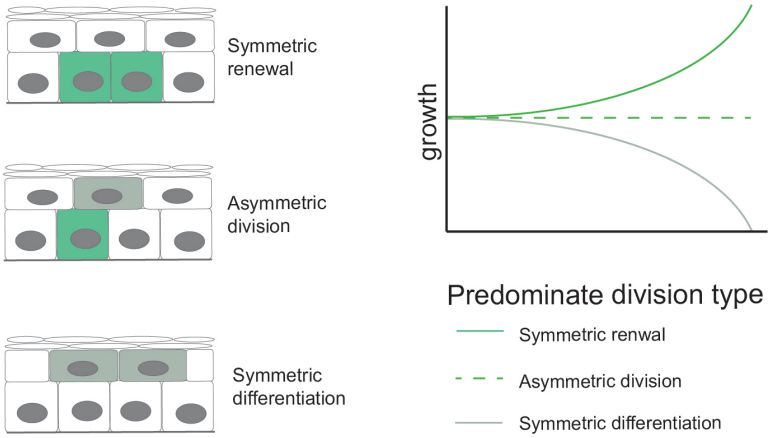

Figure 3: Progenitor cells of the epidermis undergo three types of division: symmetric renewal, asymmetric division, and symmetric differentiation. The growth potential of the epidermis changes based on the predominate division type.

The balance between renewal and differentiation is crucial in producing differentiated cells and in establishing a progenitor pool, thereby maintaining homeostasis in the epidermis. Because differentiated keratinocytes are not mitotically active and progenitor basal cells are, an asymmetric division will have a neutral effect on the growth potential of the tissue. Conversely, a symmetric renewing division will increase the size of the progenitor pool, thus increasing the renewal potential of the epidermis, while a symmetric differentiation division will decrease growth potential of the tissue (Tomasetti and Levy, 2010). This idea is important when considering normal and oncogenic growth because cells do not need to simply proliferate to develop into a tumor; they also need to renew in order to persist in a tissue. The balance between renewal and differentiation in conjunction with proliferation is what can turn a benign mutagenic event into a problematic clone, and how a tissue responds to these clones can stall or encourage tumorigenesis. It is this balance between renewal and differentiation that this study will closely analyze in order to understand oncogenic clone growth dynamics within the epidermis.

1.4 Cell behavior and the microenvironment

Cell behavior expands beyond cell-autonomous factors. The microenvironment of a cell can influence its function and fate. Cell differentiation is a tightly controlled but also a very fluid process (Blau and Baltimore, 1991; Nelson and Bissell, 2006). Evidence of this idea lies in the observation that ectodermal fates are mediated by mesodermal cues. It follows that mouse embryonic mesoderm recombined with mouse embryonic ectoderm causes the ectoderm to form normal hair follicles. However, in a striking observation, corneal epithelium from a chick recombined with mouse mesoderm induces feather development (Coulombre and Coulombre, 1971). Further research revealed this plasticity can be seen in adult cells, which are often thought to undergo irreversible fate choices. In a significant study, mammary epithelium recombined with mammary mesenchyme yielded normal mammary trees, but when mammary epithelium and salivary mesenchyme were recombined, the structure resembled a salivary tree (Sakakura et al., 1976), pointing to the fluid nature of adult cell differentiation states and the importance of a cell's environment in influencing its behavior.

The interplay of mesenchymal/ectodermal signaling can be observed in the skin. The hair follicle, which is derived from the ectoderm, needs cues from the dermal papilla—a mesenchymal structure—to continue through the hair cycle. Laser ablation of the dermal papilla arrests hair growth (Rompolas et al., 2012). Furthermore, signals from the circulatory system lead to hair cycle progression. When angiogenesis is inhibited, anagen is stalled (Mecklenburg et al., 2000). Another interaction occurs between the hair follicle and the arrector pili muscle. The $\alpha_8\beta_1$ integrin ligand, nephronectin, is produced by bulge stem cells. Accumulation of this factor in the basement membrane adjacent to the bulge leads to the recruitment of $\alpha_8\beta_1^+$ dermal cells. After interaction of $\alpha_8\beta_1^+$ and nephronectin, the dermal cells begin to express smooth muscle actin, a marker for arrector pili muscle (Fujiwara et al., 2011). Thus, an appendage of the epidermis, the hair follicle,

leads to the development of a mesenchymal tissue, the arrector pili muscle. This highlights the fact that a cell's behavior is dependent on its own cell-autonomous cues but also on those from its surrounding environment.

The microenvironment is important in development and maintenance of epidermal structure and function but also affects cancer cells. When carcinoma cells were injected into normal blastocytes, the resulting adult mice had evidence of the original cells derived from the carcinoma but their tissues were physiologically normal (Mintz and Illmensee, 1975), indicating that transferring an aggressive cancer cell to a normal environment can alter its oncogenic abilities. In another observation, mammary tumor cells differentiated if exposed to normal embryonic mesenchyme (DeCosse et al., 1973), providing another example that cancer cells respond to cues from surrounding normal tissues. The present study seeks to understand how the epidermis responds to the growth of a single oncogenic clone. It is therefore important to consider not only the interactions of the homotypic population of basal cells but also cues from the surrounding heterotypic cells.

1.5 Oncogenic growth in the epidermis

There is evidence that the epidermis can ameliorate oncogenic growth, removing cells with high fitness and returning the tissue to homeostasis. Activating β-catenin in hair follicles leads to aberrant growths, but these protrusions permanently regress over time (Brown et al., 2017). Oncogenic growth can also be suppressed via differentiation. When activating the commonly mutated PI3K-AKT pathway in murine epidermis using oncogenic Pik3ca, the resulting clones, though more proliferative than wild type cells underwent symmetric differentiation. The result was the population of progenitor cells shrank due to daughter cells differentiating (Ying et al., 2018). Because the oncogenic clones were abolished in both of these studies—the β-catenin growths

regressed and the Pick3ca clones underwent differentiation to such as extent that they were lost—the mystery of how the epidermis can control the growth of a single, persistent clone remains.

In order to answer this question we utilized a model based on oncogenic Ras, a well-studied and highly relevant oncogene. Activating mutations in Ras genes, encoding Kras, Nras and Hras, are commonly mutated in cancer (Fernandez-Medarde and Santos, 2011) and have been shown to evade rapid removal, as seen in oncogenic mutations of β-catenin and Pik3ca. Ras is membrane associated and functions in receptor tyrosine kinase (RTK) signaling, which broadly regulates a myriad of cell processes. When active, Ras is bound to guanosine triphosphate (GTP), and when inactive, Ras is bound to guanosine diphosphate (GDP). This switch between active/inactive states is regulated by GTPase activating proteins (GAPs) and guanine nucleotide exchange factors (GEFs). Specifically, GEFs assist in Ras releasing GDP, thus allowing Ras to bind GTP, a reaction that is accelerated by GAPs. Mutations in codon 12 of Ras are relevant in cancer. It is theorized that mutating codon 12 renders Ras unable to complex with GAP, making Ras unable to hydrolyze GTP (Scheffzek et al., 1997).

There are numerous Ras effectors which regulate a myriad of cell processes. Perhaps the best studied are Raf kinases which carry out Ras-Raf-Mek-Erk signaling, thereby promoting cell cycle progression. This pathway has been shown to inhibit differentiation in keratinocytes (Dajee et al., 2002). Ras signaling through another effector, phosphoinositide 3-kinase (PI3K) eventually leads to activation of Akt, which is key in fulfilling the survival characteristics of Ras. PI3K is also important in development and tumor maintenance. Mice with PI3Kα mutations, which render the protein unable to bind Ras, experience high mortality rates early in life, and those that do live to reach maturity have defective circulatory and lymphatic systems. (Castellano et al., 2013; Gupta et al., 2007). An additional Ras effector contributes to cell survival. Ras activation of Ral proteins

leads to the downstream inhibition of Foxo transcription factors, which promote cell cycle arrest (Downward, 2003).

In this study, we use oncogenic Hras ($Hras^{G12V}$) which induces clones within the IFE that not only persist but can develop into papillomas (Beronja et al., 2013). Hras is a main target in chemically-induced skin carcinomas (Quintanilla et al., 1986) and is mutated in many cancers, including 16-25% of cutaneous squamous cell carcinomas (Balmain and Pragnell, 1983; Dotto and Rustgi, 2016; Karnoub and Weinberg, 2008). $Hras^{G12V}$ activation in murine hair follicles causes malformed structures to develop, but they are corrected after completion of the hair follicle cycle, indicating that the epidermis responds to $Hras^{G12V}$ activation (Brown et al., 2017). Taken together, Hras is a relevant oncogene that has longevity in the IFE, which makes it a favorable gene to study in order to understand clonal dynamics in the epidermis.

To detect cell fate choices within clones, we employ a novel cell fate identification assay (CFI). We follow expanding $Hras^{G12V}$ clones and describe the changes in cell fates, which lead to heterogeneity in an oncogenic clone. This ultimately causes a dramatic change in renewal of the entire clone. We utilize a genetic screen to determine which Ras effector promotes differentiation and identify Rassf5 as a candidate. Finally, we show that over expression of Rassf5 leads to increased differentiation and inhibition of $Hras^{G12V}$ induced growth.

Chapter 2—Materials and methods

Animals. All mice were on a C57BL/6 or a C56BL/6-Tyr$^{c\text{-}2J}$ background including, *Hras*$^{G12V/G12V}$ (Chen et al., 2009), *Tg(K14-cre)1Efu* (Vasioukhin et al., 1999), *Gt(Rosa)26Sor*$^{tm1(eYFP)Cos/+}$ (Jackson Laboratories), and *Gt(ROSA)26Sor*$^{tm4(ACTB\text{-}tdTomato,\text{-}EGFO)Luo}$ (Jackson Laboratories). All animal experiments were conducted under approved IACUC protocols. Mice were housed and cared for in an AAALAC-accredited facility at Fred Hutchinson Cancer Research Center. Female and male animals were used in equal numbers. Randomization and blinding were not used in this study.

Cell fate identification assay. EdU (5 mg/mL, Santa Cruz) was administered via intraperitoneal injection to adult animals followed 2 hrs later by BrdU (10 mg/mL, Thermo Fisher). Animals were euthanized 24 hours after EdU injection. Head skin was removed and samples were incubated in 30mM EDTA overnight at 4^{o}C and then for 2 hours at 37^{o}C to separate dermis from epidermis. The epidermis was then gently separated from the dermis by scrapping with a scalpel, fixed for 1 hr in 4% PFA/PBS (Fisher), followed by incubations for 1 hr in 0.5% Triton/PBS (Sigma) and then 1 hr in blocking buffer (1% BSA, 1% Gelatin, 2% normal goat serum, 0.5% Triton in PBS). Next, tissues were incubated with primary chicken anti-GFP antibody overnight at 4^{o}C (to label transduced clones), and then processed for EdU expression using Click-iT technology (Invitrogen) according to the manufacturer's instructions. This was followed by a 15-minute treatment in 2N HCL (Thermo Fisher) at 37^{o}C to denature DNA and two washes in 0.1 M sodium borate/H_2O, pH 8.5. Following this quenching step, tissues were incubated in anti-chicken secondary (1:2000, Invitrogen) for 1 hr. After incubation in M.O.M. buffer (Vector Labs) for 1 hr, tissues were processed for BrdU detection, stained with 4,6-diamidino-2-

phenylindole (1:2000, DAPI; Life Technologies), and mounted in ProLong Gold (Invitrogen). Images were collected using a Zeiss LSM700 system with a Plan-Apochromat 40X/1.4 oil objective. In order to create images with enough detail to accurately score division type, Z-stacks, spanning the full thickness of the epidermis, with 1 μm slice intervals were generated. Fates were scored by determining daughter cell location (basal or suprabasal layer) and morphology (cuboidal or squamous.)

Cell cycle interval assay. Mice were injected with EdU (5 mg/mL, Santa Cruz), followed by BrdU (10 mg/mL, Thermo Fisher) two hours later. Tissues were then prepared for wholemount confocal imaging 24 hours post BrdU injection. By focusing on EdU+ only cells, we can quantify the number of cells which have completed the cell cycle within the 2 hr time frame. To calculate cell cycle division interval, we refer to EdU+ only cells as *E*. Each *E* division results in two daughter cells. Thus, the number of dividing cells in a given time frame is (*E*/2). Because only epidermal basal cells are mitotically active, we define the fraction (*F)* of basal cells which divide within a given time frame (2 hrs) to produce *E* daughter cells as $F = (E/2)/(\text{total basal cell number})$. We used this figure to extrapolate average cell cycle length (in hours) of the entire basal population (*L)* using the following ratio: $L/1 = 2 \text{ hrs}/F$. We analyzed cell cycle progression and found no differences in the length of S-phase between WT and mutant cells (Ying et al., 2018)

EdU-BrdU pulse-chase differentiation assay and renewal rate quantification. Mice were first injected with EdU (5 mg/mL, Santa Cruz), follow by BrdU 2 hrs later (10 mg/mL, Thermo Fisher). Tissues were processed 6 hours after BrdU injection. This allows for an EdU only population which has sufficient time to complete S-phase, divide, and differentiate (Ying et al., 2018). The

majority of cells divide, with only a small number (3.8%) halting their progress in G2 phase. The skin was then embedded in OCT. After sectioning, tissues were fixed in 4% PFA/PBS (Fisher), washed in 0.1% Triton/PBS (Sigma-Alrich) followed by incubation for 1 h at room temperature in blocking buffer (1% BSA, 1% Gelatin, 2% normal goat serum, 0.5% Triton in PBS). Tissues were processed for K10 detection (905401, 1:1000, BioLegend) and then processed for EdU expression using Click-iT technology (Invitrogen) according to the manufacturer's instructions. This was followed by incubation in 2N HCL (Thermo Fisher) for 30 minutes at 37°C to denature DNA, and two washes with 0.1 M sodium borate/H_2O (Carolina), pH 8.5 for 15 minutes. Tissue sections were then incubated in M.O.M. buffer (Vector Labs) for 1 h and processed for BrdU detection followed by mounting in ProLong Gold (Invitrogen). Slides were imaged using a Zeiss LSM700 system with a Plan-Apochromat 40X/1.4 oil objective. Rate of renewal was calculated using the following formula: rate of renewal = (EdU+/K10- cells) / (total number of EdU+ cells).

Proliferation assay. Head skin was processed using the CFI assay protocol, described above. To determine proliferation rate, we calculated the proportion of EdU+ progenitor cells within transduced clones.

Immunofluorescence. The following primary antibodies were used: chicken anti-GFP (ab13970, 1:1000; Abcam); mouse anti-BrdU (MoBU-1, 1:100; Invitrogen); rabbit anti-K10 (Poly19054, 1:1,000 BioLegend); rabbit anti-RFP (6000-401-379, 1:1000; Rockland), rat anti-Nidogen (sc-33706, 1:1000; Santa Cruz Biotechnology). 8 μm tissue sections were fixed in 4% PFA/PBS (Fisher) for 15 minutes, washed 3x in PBS and then permeabilized in 0.1% TritonX-

100 (Sigma-Aldrich) for 15 minutes. Tissues were then incubated for 1 hr at room temperature in blocking buffer (1% BSA, 1% gelatin, 2% normal goat serum, 0.1% Triton) and then in primary antibody overnight at 4°C. Tissues were then incubated at room temperature for 1 hr with secondary antibody and mounted in ProLong Gold (Invitrogen) with or without 4,6-diamidino-2-phenylindole (DAPI; Life Technologies). Confocal images were taken on a Zeiss LSM700 system using a Plan-Apochromat 40X/1.4 oil objective. Image processing was done using Zeiss Zen and ImageJ software.

Cell packing quantification. Head skin was prepared for whole-mount confocal imaging. Images were collected using a Zeiss LSM700 system with a Plan-Apochromat 40X/1.4 oil objective. Clone area was measured using ImageJ. Cell density was calculated using the formula: clone density = (# basal cells / clone area).

Clone morphology and circularity quantification. Head skin whole-mounts were imaged on a Zeiss LSM700 system with a Plan-Apochromat 40X/1.4 oil objective. Using ImageJ, clone outlines were traced and an ellipse was fitted to each clone, using ImageJ software. The perimeter and area of the ellipse was measured using ImageJ. Circularity was calculated using the following equation: circularity = $4\pi(\text{area} / \text{perimeter}^2)$.

Western Blot. Head skin from E18.5 animals was incubated in 2mg/mL dispase (Thermo Fisher Scientific) at 37ºC for 1 hr to separate dermis from epidermis. The epidermis was then digested in RIPA buffer with phosphatase and protease inhibitor cocktails (Santa Cruz Biotechnology) for 30

minutes on ice followed by sonication. Supernatants were assayed for protein concentration using the Pierce BCA Protein Assay Kit (Thermo Fisher). Western blotting was performed using a Novex system (Invitrogen). Membranes were incubated with primary antibody overnight and then incubated with HRP-conjugated secondary antibodies (1:2000, Jackson Immunoresearch) for 1 hr at room temperature. Membranes were developed using SuperSignal West Femto Maximum Sensitivity Substrate (Thermo Fisher). Chemiluminescent signals were detected using an Odyssey Fc system (LI-COR). The following primary antibodies were used: rabbit anti-Nore1A (PAS17071, 1:1000; donated by G. Clark), mouse anti-GAPDH (60004-1-Ig, 1:2000; Proteintech).

***In* vivo genetic screens.** Head skin of E18.5 mice was collected and digested in 2mg/mL dispase (Thermo Fisher Scientific) at 37^{o}C for 1 hr to separate dermis from epidermis. Epidermal tissue was then digested in 0.25% trypsin (Life Technologies) for 30 minutes to isolate single cells. Cells were labeled with CD49f/α_6-integrin-PerCP (1:50; BioLegend) and purified using fluorescence activated cell sorting (FACS) using BD FACSAria II (BD Biosciences). Genomic DNA was extracted using DNeasy Blood & Tissue Kit (Qiagen). Barcode pre-amplification, sequencing and data processing using the Deseq2 program were performed as previously described (Ying et al., 2018).

Lentiviral constructs. A mouse Rassf5 expression construct (Addgene) was cloned into tdTomato-C1 vector at EcoRI/SmaI sites. Rassf5-tdT was then cloned into a modified pLX Cre EF1 vector (Ying et al., 2018) using the Zero Blunt TOPO kit (Invitrogen). RNA interference-mediated gene depletion was achieved using pLKO1 shRNA vectors from the mouse TRC1.0

shRNA library (Sigma-Aldrich). pLKO-Cre vectors were used to generate Cre-shRNA expression constructs (Beronja et al., 2013; Beronja et al., 2010).

Lentiviral production. 293FT cells were transfected using the calcium phosphate method with pLKO.1, pMD2.G and psPAX2 (Addgene). After 48 hrs viral supernatant was collected and filtered using a Stericup-HV PVDF 0.45μm filter (Millipore). Concentration was carried out in two steps: first using a Centricon Plus-70 100 KDa centrifugal filter (Millipore) and second by ultracentrifugation. Virus was reconstituted and then injected into E9.5 embryos.

Ultra-sound guided in-utero injections. Pregnant females carrying E9.5 embryos were anesthetized with isoflurane (MWI Veterinary Supply Company) and injected as previously described (Beronja and Fuchs, 2013; Beronja et al., 2010). Each embryo was injected with ~1ul of lentivirus. A max of six embryos were injected per litter. Females were monitored for 30 minutes after the surgery to ensure recovery.

mRNA quantifications. Total RNA was isolated from cultured keratinocytes or from E18.5 FACS-sorted epidermal cells using RNeasy Plus Mini Kit (Qiagen). Complementary DNA was generated from 1 μg of total RNA using the iScript Reverse Transcription Supermix (Bio-Rad). Quantitative PCR was performed with SYBR Green PCR Master Mix (Thermo Fisher) and with gene specific and Rpl16 control primers.

Intravital imaging using two-photon microscopy. An LSM 780 multiphoton, laser scanning confocal microscope (Zeiss) was used in intravital imaging. Details of the technique have been previously described (Rompolas et al., 2013). Mice were anesthetized and further immobilized using a custom device so that the head skin could be imaged without interfering vibrations. GFP and Tomato signals were excited and captured using a 940-nm laser.

Papilloma growth quantifications. Control and $Hras^{G12V}$ animals were transduced with LV-Cre containing constitutively expressing shRNA against scrambled control or test Rassf5 shRNAs. Transduction was confirmed at p21 via Cre-reporter activation and animals were monitored for 12 weeks. Papillomas were scored positive when larger than 3 mm in diameter and were measured weekly along their long and short axis using a digital caliper. Papilloma volumes were calculated using the formula V=(p/6)x(LxWxD) (Tomayko and Reynolds, 1989), normalized to initial papilloma volume, and expressed as fold-change over time.

Statistical information. All experiments were performed at least in triplicate, and all quantitative data are expressed as mean ± standard deviation. Differences between conditions were analyzed in Prism 7 (GraphPad Prism) using Student's t-test. Significant differences were considered when p value <0.05.

Chapter 3—Expression of activated Hras^{G12V} promotes progenitor cell renewal in adult skin epithelium.

3.1 Intra-vital imaging quantifies renewal rate in individual progenitor cells

In order to explore the immediate effect of single cell activation of a potent oncogene on progenitor cell fate, we employed an *Hras$^{lox\text{-}WT\text{-}stop\text{-}lox\text{-}G12V}$* (*Hras$^{ll\text{-}G12V}$*); *Rosa26$^{mT/mG}$* (*R26*) mouse (Figure 4A) (Chen et al., 2009; Muzumdar et al., 2007). We transduced the epidermis of mid-gestation embryos, using ultrasound-guided intra-amniotic injection (Beronja et al., 2013; Beronja et al., 2010), with lentivirus containing inducible Cre-recombinase (LV-CreER) at clonal density (Figure 4A). This model allowed for: (i) Tamoxifen-induced recombination in the adult epidermis, at a dose determined to result in sporadic single cell activation events; (ii) expression of an oncogenic form of Hras (Hras^{G12V}) from its endogenous promoter, ensuring both physiological mRNA/protein levels and regulatory control; and (iii) stable labeling of activated cells by Cre-mediated replacement of membrane-associated (m) Tomato fluorescent protein with mGFP (Figure 4A). We induced recombination at postnatal day 19 (P19) and imaged tissues 48 hours later, allowing sufficient time for individual progenitor cells to divide and for the resulting two daughter cells to commit to either basal progenitor or suprabasal differentiated cell fate (Figure 4B,C) (Ying et al., 2018). Using intravital two-photon microscopy (Rompolas et al., 2013) we were able to image through the full thickness of the epidermis, identify the differentiation state of each of the two daughter cells derived from a single activated cell at P21, and score every progenitor cell division that occurred as either symmetric renewal, asymmetric division, or symmetric differentiation (Figure 4C,D).

Analysis of control (*R26*) head skin epidermis showed that asymmetric divisions, once considered the predominant division type of epidermal progenitors, occurred in approximately 44%

of cases, and that symmetric renewal was nearly perfectly balanced by symmetric differentiation (29% vs. 27%) (Figure 4E). In contrast, we observed a striking change in progenitor division type following expression of $Hras^{G12V}$, with a significant increase in symmetric renewal (48%) and a significant decrease in symmetric differentiation (10%) (Figure 4E). We used the observed frequency of cell division types in control and oncogene-expressing epidermis to calculate the rate of progenitor renewal, which measures the proportion of new daughter cells that maintain progenitor potential (Ying et al., 2018). Epidermal progenitors in the control tissue had a renewal rate of ~0.5 (Figure 4F). Such a rate is expected to maintain a stable population of basal progenitors long-term and ensure neutral tissue growth. $Hras^{G12V}$-expressing progenitors showed higher renewal rate of 0.69, which implies that oncogenic Hras, unlike single cell expression of activated Pik3ca (Ying et al., 2018), promotes progenitor cell renewal. It also suggests that in contrast to loss of cellular fitness we observed in oncogenic Pik3ca epidermis (Ying et al., 2018), $Hras^{G12V}$-expressing progenitors could support expansion and long-term maintenance of oncogenic clones.

3.2 $Hras^{G12V}$ growth is inhibited by unknown mechanisms

Apoptosis and senescence were not significantly different between wild type and oncogene expressing epidermis (Figure 5A,B), but $Hras^{G12V}$ cells have faster renewal and proliferation rates (Figures 4F,5C), which we hypothesize leads to rapid expansion of $Hras^{G12V}$ clones. We tested this by direct imaging and quantification of basal cells in control and $Hras^{G12V}$-expressing clones at 24 weeks (Figure 5D,E). At this time point, $Hras^{G12V}$ clones are significantly larger than WT clones but smaller than expected, which suggests that additional mechanisms of growth suppression are at play to curtail growth potential of $Hras^{G12V}$ progenitor cells.

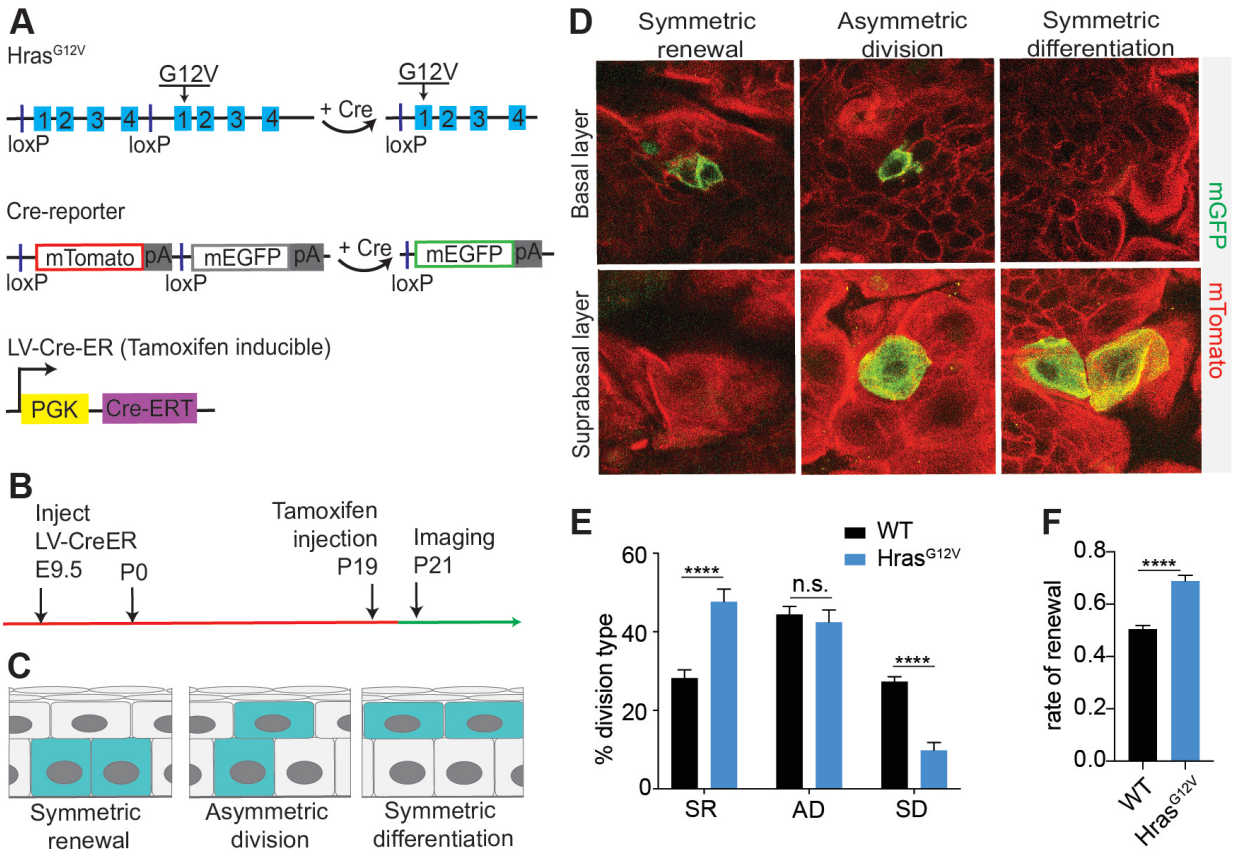

Figure 4 Hras^{G12V} induces progenitor cell renewal in single cells. **(A)** Schematic of *Hras$^{ll\text{-}G12V}$* and *R26* mice. *Hras$^{ll\text{-}G12V}$* mouse changes expression of WT-Hras allele to mutant-Hras allele upon addition of Cre. *R26* mouse changes expression of mTomato to mGFP after Cre activation. CreER expression is induced by tamoxifen. **(B)** Schematic of single cell induction and imaging experiment. **(C)** Epidermal progenitor cells can undergo three distinct division types. **(D)** Representative images of basal progenitor cell divisions in Cre-activated *R26* epidermis captured using intra-vital imaging. Scale bar is 10 μm. **(E)** Quantification of division choices of single cells in adult epidermis. **(F)** Rate of renewal significantly increases in single Hras^{G12V} progenitor cells. For **E,F** statistics were based on n≧3 animals for each condition; the center line represents the mean; errors bars represent the s.d. Two-tailed Student's t-test was used. **** denotes p value <0.0001

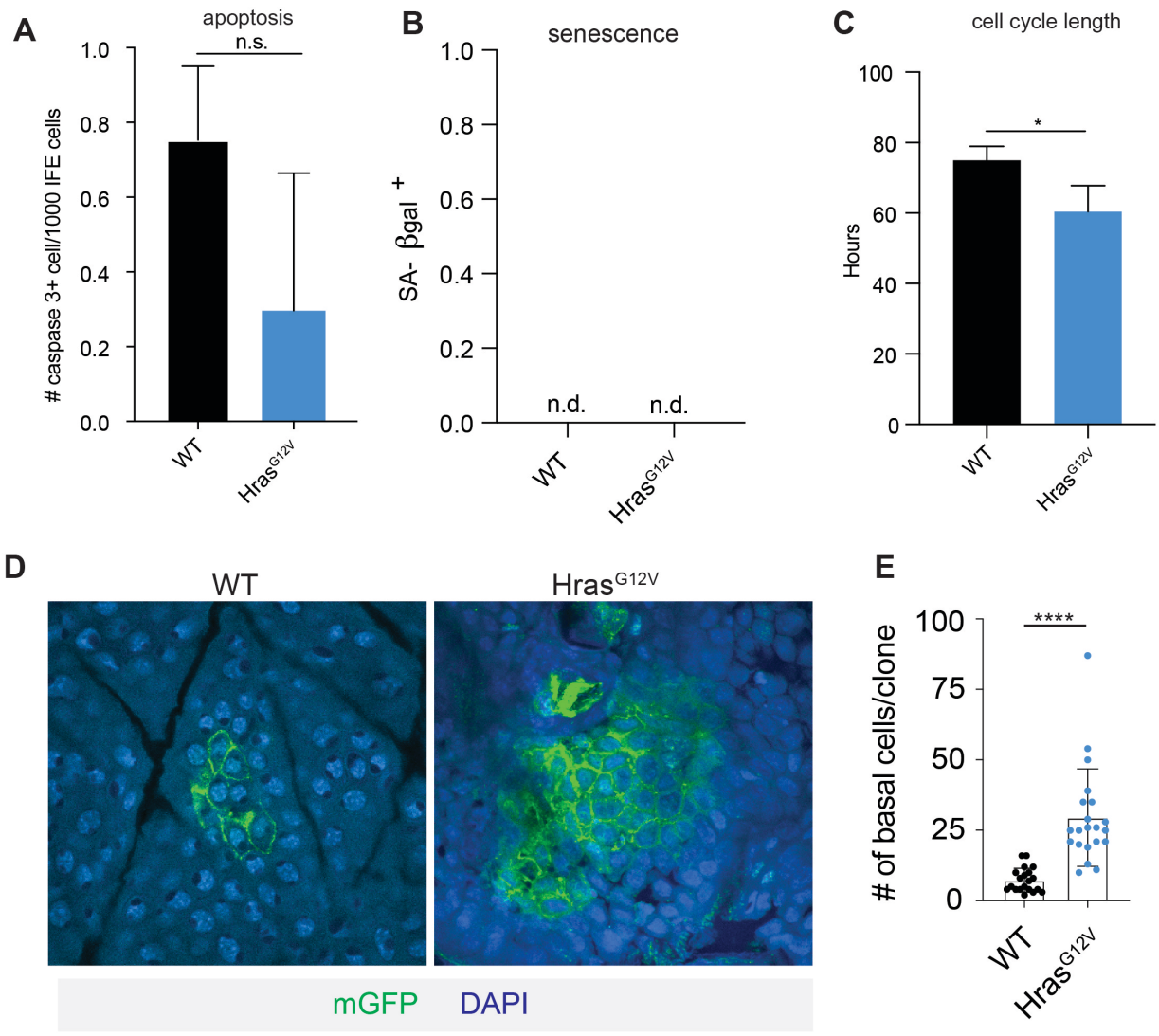

Figure 5 Additional mechanisms are required to stall oncogenic growth. **(A)** Quantification of caspase 3^+ cells in E18.5 epidermis. **(B)** Quantification of β-galactosidase associated cells in E18.5 epidermis. **(C)** Quantification of average time between consecutive cell division events in adult WT and $Hras^{G12V}$ epidermis. **(D)** Representative images of basal cells of WT and $Hras^{G12V}$ clones at 24 weeks. Scale bar is 10 μm. **(E)** Quantification of basal cell numbers in WT and $Hras^{G12V}$ clones at 24 weeks. For **(A-C)** statistics were based on n≧3 animals for each condition. For **(E)** statistics were based on 20 clones from n=3 animals. The center line represents the mean and errors

bars the s.d. Two-tailed Student's t-test was used. n.s. denotes not significant. * denotes p value <0.05; **** denotes p value <0.0001

Chapter 4—Novel cell fate identification assay describes heterogeneity in oncogenic clones

4.1 Development of an assay for quantification of progenitor cell fates in vivo.

Next, we set to determine if high proliferation and renewal rates were sustained in $Hras^{G12V}$ clones over time. While proliferation could be measured using standard approaches, a simple and broadly accessible assay that can directly score progenitor cell fate choice was lacking. We recently employed an EdU/BrdU differentiation assay (Ying et al., 2018) that allowed us to analyze progenitor daughter cells as a population and estimate tissue renewal rate based on their relative expression of differentiation marker Keratin 10 (K10). Here we modified this approach to develop a cell fate identification (CFI) assay, which allows us to classify each progenitor cell division event as asymmetric, symmetric renewal or symmetric differentiation.

We first gave animals a pulse of EdU then processed the tissue for standard confocal imaging 30 minutes later (Figure 6A). We observed EdU^+ labeling of single cells throughout the tissue that was restricted to the progenitors in the $K10^-$ basal layer (Figure 6B). Following the EdU pulse with administration of BrdU 2 hrs later (Figure 6A) resulted in the appearance of sporadic $EdU^+/BrdU^+$ single cells and a population of $EdU^+/BrdU^-$ cells, in which ~15% of cells had already divided but not differentiated (Figure 6B). By 24 hrs all $EdU^+/BrdU^-$ cells were found as doublets and in both basal ($K10^-$) and differentiated $K10^+$ suprabasal layers (Figure 6B). These EdU^+-only cells represents the daughters of progenitor cells that have exited the S-phase within a defined period (0-2 hrs), and have been given sufficient time to show their differentiation state. By keeping the epidermis intact through processing and immunofluorescence staining, we are able to image every EdU^+-only doublet in tissue whole-mounts and assign daughter cell fates based on cellular morphology (cuboidal vs. flat) and location in the tissue (basal vs. suprabasal; Figure 6C).

We next compared the frequency of cell division types in control epidermis as measured by CFI with that obtained using intravital two-photon imaging of LV-CreER transduced single cells (Figures 4D, 6D). We observed no significant differences between the two assays, suggesting that in CFI we have a valid and direct method for quantifying cell fate decision within the adult murine epidermis.

4.2 Epidermal expression of Hras^{G12V} results in dynamic changes in progenitor cell fate choice.

To investigate how proliferation and cell fate choice may evolve in Hras^{G12V} cells over time, and account for relatively restricted growth of oncogene-expressing clones (Figure 5D,E), we measured their proliferation and renewal rates. We lineage traced control and Hras^{G12V} clones initiated from a single cell at P21 and collected tissues at two-week intervals (Figure 6A). We observed that oncogenic clones undergo more symmetric renewal initially, but by eight to ten weeks of growth the proportion of symmetric renewal divisions decreased and returned to rates observed in wild type clones (Figure 6B). Early increase in symmetric renewal was accompanied by reduction in the rates of symmetric differentiation and asymmetric divisions, which also returned to wild type levels by eight to ten weeks (Figure 6C,D). From the observed frequency of cell division types we calculated the rate of progenitor renewal. The wild type progenitors maintained a renewal rate of ~0.5 throughout the duration of the study, consistent with a neutral growth potential of a homeostatic tissue (Figure 6E). In contrast, the Hras^{G12V}-expressing progenitors showed an increase in renewal rate to ~0.70-0.85 in the initial eight weeks, but then fell to ~0.55 over the next several weeks as differentiating and asymmetric cell divisions increased (Figure 6E).

We also measured proliferation rates in control and Hras^{G12V} clones over the same period, and observed that while oncogene expressing cells had a higher rate of EdU incorporation than wild type, the rates were largely stable over 24 weeks (Figure 6F). The higher rate of proliferation and renewal lead to sustained expansion of Hras^{G12V} clones (Figure 6F). Together, this suggests that clonal expansion driven by a single oncogenic lesion is dependent on the cellular mechanisms of progenitor proliferation and renewal, with fluctuating rates of cell fate choice being the dominant determinant of growth dynamics.

4.3 Emerging heterogeneity in expanding Hras^{G12V} clones impacts progenitor renewal behavior.

Intrigued by the observed switch from highly renewing to more balanced cell fate choices we revisited oncogene-expressing clones early (weeks 2 and 4) and late (weeks 10 and 24) following single-cell Hras^{G12V} activation (Figure 7). We used confocal microscopy of epidermal whole mounts to observe individual YFP+ clones, and image processing to distinctly visualize their progenitor compartment (Figure 8A). Based on evidence that cell packing can have profound effect on delamination (Lee et al., 1998; Poumay and Pittelkow, 1995), we first compared clonal cell density between early and late Hras^{G12V}-expressing cells (Figure 8B). We observed that cell density increases between two and four weeks but then remains stable as highly renewing clones transition to more differentiating clones. This lack of temporal correlation suggested that cell density does not drive the switch in progenitor renewal.

We noted that the shape of expanding Hras^{G12V} clones appeared to be relatively round, irrespective of their age and size (Figure 8C). Indeed, this was confirmed through analysis of clone circularity (Figure 8D) and further implied that, as clones expand, their area increases at a greater rate than their circumference. This suggested that time-dependent increase in clone size may be

accompanied by a change in its overall composition in respect to the ratio of 'edge' cells, found along the circumference of the clone and in contact with WT neighbors, to 'inner' cells, found in the center of the clone and in contact with other $Hras^{G12V}$-expressing progenitors. To test this, we quantified the number of edge and inner cells in $Hras^{G12V}$ clones and observed that while both populations enlarged in absolute terms (Figure 8E), the relative abundance of inner cells increased from 14 to 45% and edge cells decreased from 86 to 55% over time (Figure 8F). Therefore, as $Hras^{G12V}$ clones expand, their composition changes in a potentially profound way. The heterotypic (WT/$Hras^{G12V}$) environment of the edge cells could influence them to behave differently than the homotypic ($Hras^{G12V}$/$Hras^{G12V}$) inner cells.

Using CFI assay we analyzed 10-week-old $Hras^{G12V}$-clones and observed that while the rate of homeostatic asymmetric divisions was similar between edge and inner cells, they significantly differed in the ratio of growth regulating symmetric fate choices (Figure 8G). Whereas edge cells underwent significantly more symmetric renewing divisions, inner daughter cells more often chose differentiated cell fates. From observed division types we extrapolated the renewal rate and established that edge cell population maintains progenitor renewal rate consistent with growth expansion (0.69) while inner population is below the 0.5 threshold required for stasis, and therefore in a state of progenitor loss (Figure 8H). Taken together, our data suggest a new model for how growth of oncogene-expressing cells becomes restricted to ensure normal function despite accumulation of cancer driving genes. According to it, a single $Hras^{G12V}$ cell initially undergoes a rapid expansion, but after several weeks, a shift in renewal driven by intra-clone heterogeneity decreases the rate of clone expansion until a point of near homeostasis. Even though the inner core of the clone is pro-differentiation, the clone does not collapse because it is maintained by the pro-renewal edge (Figure 8I). It also suggests the existence of a currently

unknown molecular mechanism that regulates dynamic cell fate choice. Such a mechanism could explain how tissues can remain phenotypically normal while maintaining a high mutation burden throughout an individual's life.

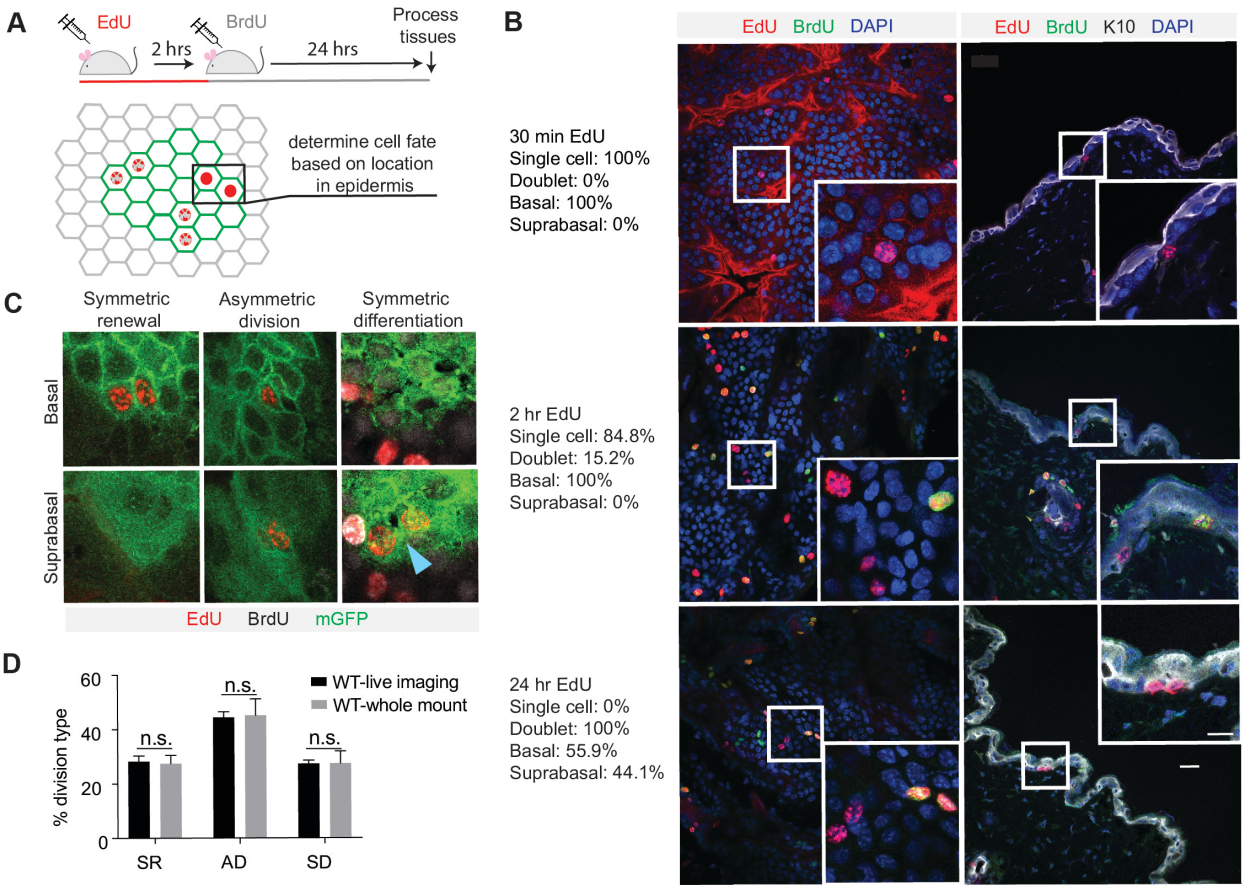

Figure 6 CFI assay specifically identifies epidermal progenitor fate choices. **(A)** Schematic of CFI assay. EdU-only cells are assessed for location in epidermis (basal or suprabasal layer) as indicator of cell fate choice. **(B)** Representative images of EdU and BrdU positive cells, 30 mins, 2.5 hrs and 24 hrs post EdU injection. Cells at the 24-hour time point are fully committed to progenitor or differentiated fate. Scale bar is 25 μm. Inset scale bar is 10 μm. **(C)** Representative images of cell divisions as seen in CFI assay. Blue arrow marks symmetric differentiation division. **(D)** Cell fate choices scored by CFI assay are not significantly different from cell fate choices scored via direct intra-vital imaging.

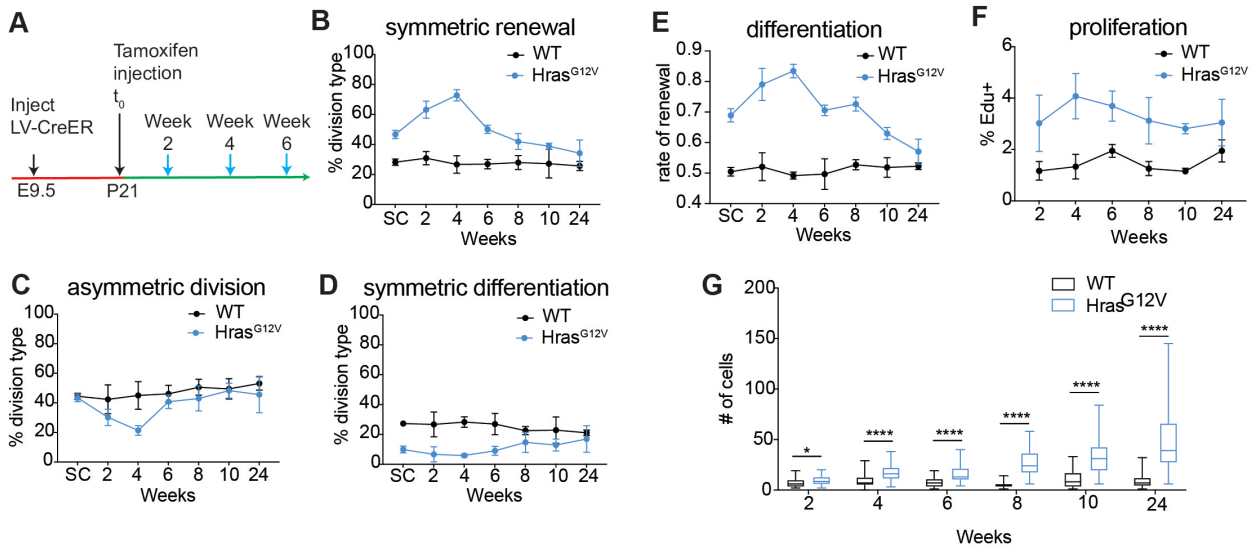

Figure 7 CFI assay reveals dynamic changes in progenitor renewal in expanding Hras^{G12V} clones. **(A)** Schematic of clone activation. Tissues were processed in 2-week intervals following tamoxifen injection (blue arrows). **(B-D)** Division choices of progenitor cells in activated clones. **(E)** Rate of renewal in Hras^{G12V} and WT clones initially differs significantly, but as Hras^{G12V} clones reach 24 weeks, renewal rates drop to near-homeostatic levels. **(F)** EdU-incorporation over 2 hrs in WT and Hras^{G12V} epidermis. **(H)** Hras^{G12V} clones expand significantly over time. For **B-F,H** statistics were based on n≧3 animals for each condition; the center point represents the mean; errors bars represent the s.d. Two-tailed Student's t-test was used. * denotes p value <0.05; **** denotes p value <0.0001

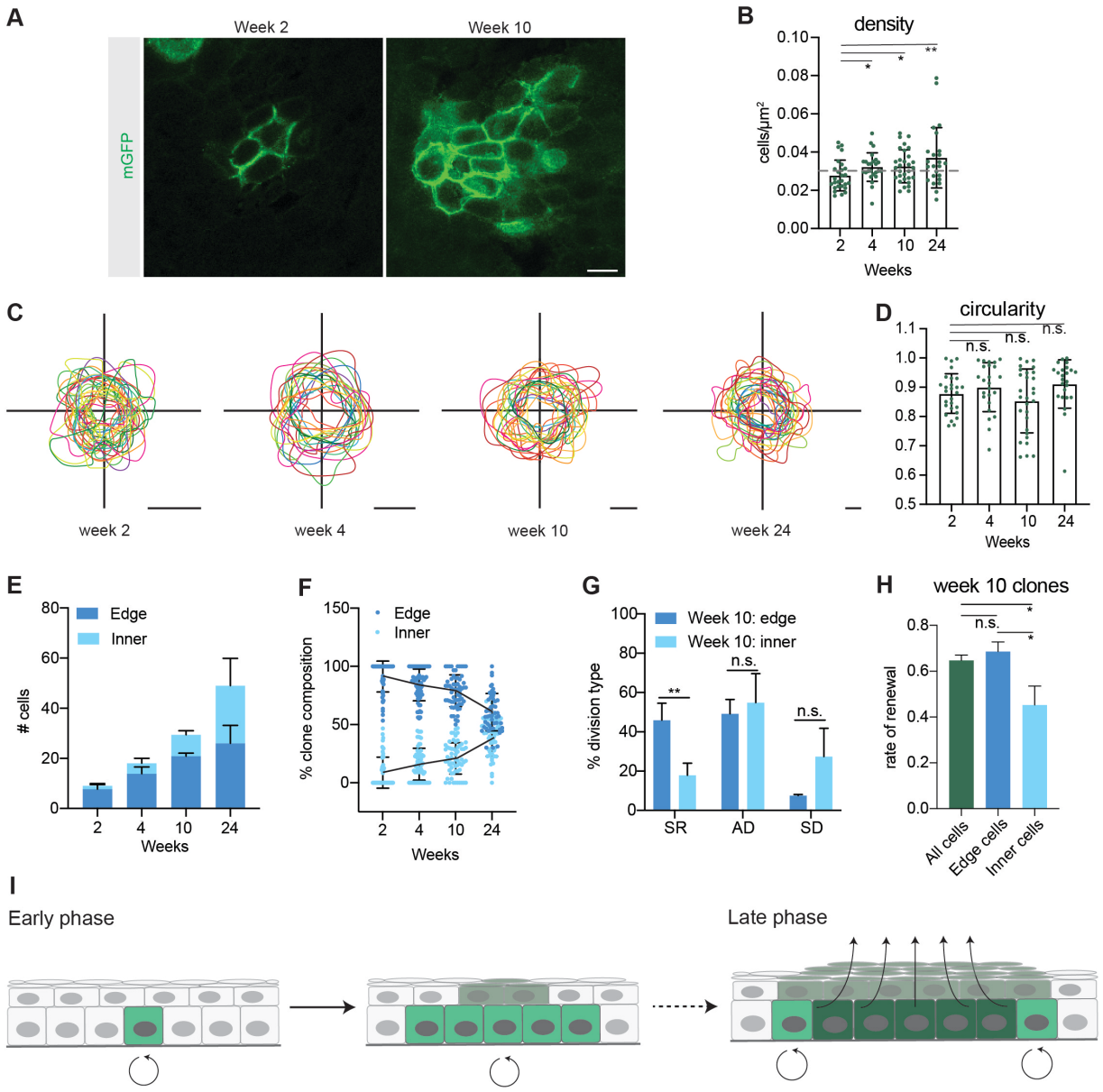

Figure 8 Hras^{G12V} clones develop intra-clone heterogeneity over time. **(A)** Representative images of basal cell population of Hras^{G12V} clones at week 2 and week 10. **(B)** Density of individual Hras^{G12V} clones. Dashed gray line represents average density in WT clones. **(C)** Outlines of individual Hras^{G12V} clones show a circular morphology. Scale bars are 25 μm. **(D)** Quantification of circularity of individual Hras^{G12V} clones. **(E)** Quantification of edge cells and inner cells in Hras^{G12V} clones. **(F)** Proportion of edge cells in Hras^{G12V} clones decreases as the clone expands. **(G)** Division choices of inner cells and edge cells in week 10 Hras^{G12V} clones. **(H)** Rate of renewal

in week 10 $Hras^{G12V}$ clones. **(I)** Early phase $Hras^{G12V}$ clones expand. In contrast, the inner region of late phase $Hras^{G12V}$ clones undergo high rates of differentiation but the clone does not collapse because the edge cells are more renewing and compensate for the inner cells. For **(B,D)** each dot represents a single clone. For **(E-H)** statistics were based on n≧3 animals for each condition; the center point represents the mean; errors bars represent the s.d. Two-tailed Student's t-test was used. * denotes p value <0.05; n.s. denotes p value >0.05.

Chapter 5—Rassf5 promotes differentiation in the epidermis and can prevent papilloma development

5.1 Functional screen identifies Hras effector Rassf5 as a mediator of cell fate choice.

We have previously shown that developing epidermis is a powerful system to conduct large-scale genetic screens and identify physiological regulators of distinct cellular processes, including progenitor renewal and differentiation (Beronja et al., 2010; Ying et al., 2018). We next set out to test if the dynamic impact of $Hras^{G12V}$ on progenitor renewal in adult skin can be recapitulated in oncogene-expressing embryonic epidermis. We first injected low titer LV-Cre (Beronja et al., 2010), encoding a constitutively active Cre recombinase, into control (*R26*) and test (*Hras*$^{ll\text{-}G12V}$; *R26*) embryos at E9.5 (Figure 9A). At E18.5, we confirmed that epidermis was transduced at clonal density (Figure 9A,B), and used EdU/BrdU differentiation assay to quantify renewal rate in YFP^{+} clones (Ying et al., 2018). We observed that progenitor renewal rates were high (~0.75), and not significantly different between control and test clones (Figure 9C). We next transduced mice with high titer LV-Cre, which resulted in broad areas of $Hras^{G12V}$ activation by E18.5 (Figure 9A,B). We quantified progenitor renewal under large field expression of $Hras^{G12V}$ and discovered a significant rate reduction (0.76 vs. 0.57; P value <0.001; Figure 9C). We also used K14-Cre transgenic mice to generate E18.5 epidermis with uniform field activation of $Hras^{G12V}$ (Figure 9A,B), and observed that the tissue's progenitor renewal rate (0.56) showed no difference between LV-Cre and K14-Cre induced fields (Figure 9C). Our data imply that a field of progenitor cells that ubiquitously express $Hras^{G12V}$ more often gives rise to differentiated daughter cells, and this correlates with the changes we see develop over time in adult $Hras^{G12V}$ clones. They also suggest that we may be able to use our E18.5 screening platform to uncover the mechanism of how activated $Hras^{G12V}$ induces differentiation.

We generated a library of short hairpin RNAs (shRNAs) targeting 28 known downstream effectors of Ras signaling. We combined 4-5 shRNAs targeting each gene into a single pool of 135 constructs, made a lentivirus titrated to result in MOI≤1, and transduced control and test E9.5 epidermis via ultrasound-guided in utero microinjection (Figure 9D). We collected the epidermis at E18.5, isolated the keratinocytes and separated them into basal (α_6 Itg^{high}) and suprabasal (α_6 Itg^{low}) populations. We reasoned that if an shRNA is enriched in the basal layer, it would imply that the corresponding gene was a negative regulator of progenitor renewal, while suprabasal enrichment would be consistent with depletion of a renewal promoter. We quantified relative abundance of shRNAs in two populations using BWA and quantified significant basal/suprabasal enrichment using DeSeq2 (Love et al., 2014; Ying et al., 2018). Genes were scored as screen hits if at least two shRNAs showed significant and consistent enrichment, as before (Beronja et al., 2013).

Our screen in wild type epidermis did not identify any Hras effector enrichment in basal or suprabasal cells (Figure 9E), suggesting that in normal development Hras signaling is not a significant regulator of progenitor cell fate choice. In contrast, the screen in $Hras^{G12V}$-expressing epidermis identified shRNAs targeting Rassf5 and Pik3ca as significantly enriched in basal cells (Figure 9F), consistent with their putative role as negative regulators of $Hras^{G12V}$-mediated progenitor cell renewal. We were gratified by this result as our lab has previously shown that activated Pik3ca can drive progenitor differentiation in the epidermis (Ying et al., 2018). We next set out to test our top hit Rassf5, as a candidate mediator of oncogene-induced differentiation.

5.2 Rassf5 mediates Hras-dependent reduction in progenitor cell renewal.

Rassf5, also known as Nore1a, is a Ras effector containing a Ras Association (RA) domain which directly binds to activated Ras (Vavvas et al., 1998). Like other RA domain family (RASSF)

members, Rassf5 lacks enzymatic activity and is often epigenetically silenced in cancer (Donninger et al., 2016). Notably, Rassf5 is methylated in the majority of esophageal and head and neck squamous cell carcinomas (Guo et al., 2015; Steinmann et al., 2009) and has been shown to inhibit Ras growth via senescence (Donninger et al., 2015) and apoptosis (Elmetwali et al., 2016; Park et al., 2010). To discern if Rassf5 also regulates progenitor cell fate choice and is critical to $Hras^{G12V}$-mediated differentiation, we first identified three independent shRNAs which depleted target mRNA by ~70% in keratinocytes. We quantified Rassf5 expression in $Hras^{G12V}$-expressing epidermis at E18.5 and discovered that both its transcript and protein were elevated relative to wild type control, indicating that activated $Hras^{G12V}$ can promote Rassf5 expression (Figure 10A,B).

To test if Rassf5 is necessary for increased differentiation under conditions of field activation of $Hras^{G12V}$, we generated lentiviral constructs for concomitant expression of Rassf5 shRNAs and constitutively active Cre (LV-Cre-sh*Rassf5*; Figure 7C). We first introduced them into *Hras*$^{ll\text{-}G12V}$; *R26* epidermis at high MOI, isolated GFP+ cells by FACS and observed a significant potential to counter $Hras^{G1V}$-driven Rassf5 expression *in vivo* (Figure 10A,B). We next transduced control and *Hras*$^{ll\text{-}G12V}$; *R26* epidermis with high-titer LV-sh*Rassf5*-Cre, collected broadly infected tissue at E18.5 and performed EdU/BrdU differentiation assay (Figure 10D). Our data show that Rassf5 depletion in large $Hras^{G12V}$-expressing clones leads to a significant increase in progenitor renewal rate, with three independent shRNAs demonstrating the same effect (Figure 10E). This signifies that Rassf5 is necessary for $Hras^{G12V}$-induced progenitor cell differentiation. We also observe increased renewal in control epidermis with one out of three shRNAs we used, which suggest that Rassf5 may have a more general ability to regulate progenitor cell renewal (Figure 10D).

To test if Rassf5 is sufficient to promote progenitor cell differentiation we focused on small $Hras^{G12V}$ clones that we demonstrated do not show increased differentiation (Figure 10C). We generated a lentivirus to simultaneously express Cre recombinase and Rassf5 open reading frame (ORF) fused to a tdTomato (LV-Cre-*Rassf5*-tdT), allowing for clonal oncogene activation and visualization of transgene expression (Figure 10E). We transduced $Hras^{ll\text{-}G12V}$; *R26* mice with similar low titers of LV-Cre and LV-Cre-*Rassf5*-tdT, and readily observed numerous epidermal clones at E18.5 epidermis. We noted a dramatic difference in their shape, with Rassf5-expressing clones appearing more triangular in cross section (Figure 10F), consistent with either a significant loss of basal progenitors or expansion of the suprabasal differentiated cell compartment. Whole mount imaging further implied that Rassf5-expressing $Hras^{G12V}$ clones were composed of fewer basal and relatively more suprabasal cells (Figure 10G). We analyzed clone composition and observed that Rassf5 promotes significant reduction in basal cell numbers and significant increase in the suprabasal to basal surface area (Figure 10H,I). Together this suggests that Rassf5 is sufficient to promote progenitor cell differentiation in $Hras^{G12V}$-expressing epidermis.

5.3 Overexpression of Rassf5 prevents papilloma development

Knowing that Rassf5 promotes differentiation, we sought to determine whether it can influence papilloma development. Mice develop papillomas several weeks after activation of oncogenic Hras (Beronja et al., 2013). Notably, $Hras^{G12V}$ mice overexpressing Rassf5 formed significantly fewer papillomas during the study period, suggesting that Rassf5's pro-differentiation action is sufficient to prevent papilloma formation (Figure 11B). Conversely, all $Hras^{G12V}$ and $Hras^{G12V}$; shRassf5 mice developed papillomas (Figure 11A). However, the results of Rassf5 knockdown on overall papilloma burden per animal and rate of papilloma growth were dependent

on the specific shRNA (Figure 11B,C). Ultimately, the effect of Rassf5 knockdown on papilloma growth is undetermined but overexpression of Rassf5 can prevent papilloma formation.

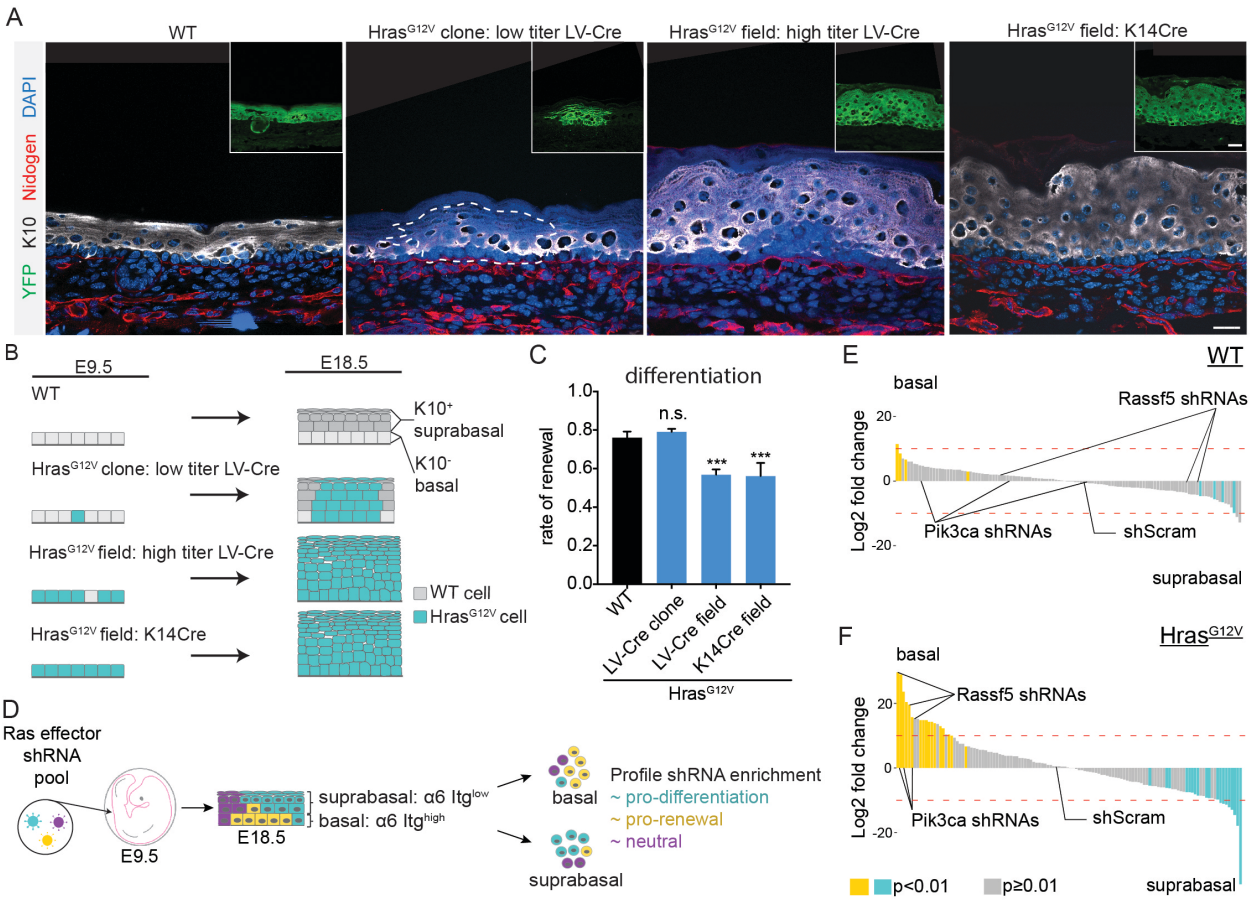

Figure 9 Hras^{G12V} induced differentiation is replicated in E18.5 epidermis and serves as the basis for *in vivo* genetic screen **(A)** Representative images of clonal and field activation of Hras^{G12V} in developing epidermis. Scale bar is 25 µm. Inset scale bar is 25 µm. **(B)** Hras^{G12V} expression can be induced with LV-Cre (high or low titer) or K14-Cre. Changes in Hras^{G12V} expression yield differences in tissue hyperplasia. **(C)** Rate of renewal decreases in tissues which broadly express Hras^{G12V} (LV-Cre field and K14Cre field)**. (D)** Diagram of shRNA screen methodology. A lentiviral pool targeting Ras effectors was injected into E9.5 embryos. The epidermis was harvested at E18.5, digested into single cells and separated by FACS based on low or high expression of α6 Itg. Each population was profiled for shRNA enrichment. **(E,F)** Needle plots of shRNA's enriched in basal layer compared to suprabasal layer in WT and Hras^{G12V} epidermis. shRNAs that are enriched in basal layer (α6 Itg^{high} population) relative to suprabasal layer (α6

Itg^{low} population) inhibit differentiation. The indicated shRNAs are candidate (Rassf5) or validated (Pik3ca) regulators of Hras^{G12V} induced differentiation. For **(C,E,F)** statistics were based on n≧3 animals for each condition; the center point represents the mean; errors bars represent the s.d. Two-tailed Student's t-test was used. n.s. denotes p value >0.05. *** denotes p value <0.001.

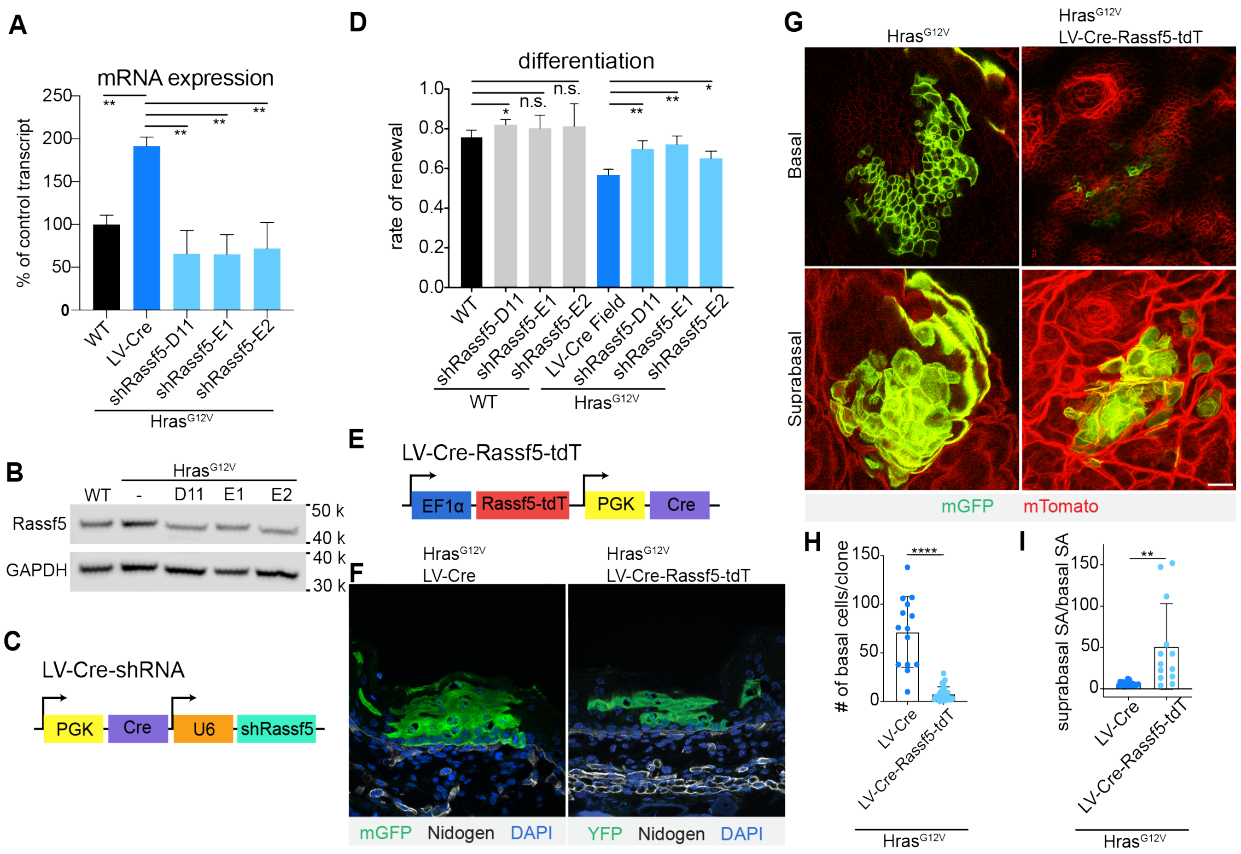

Figure 10 Rassf5 is a necessary and sufficient driver of Hras^{G12V} induced differentiation. **(A)** Rassf5 mRNA is increased in isolated Hras^{G12V} E18.5 basal cells. shRNAs targeting Rassf5 efficiently knock down transcript expression. **(B)** Immunoblot of Rassf5 expression in Hras^{G12V} E18.5 epidermis **(C)** LV-Cre-shRassf5 construct for simultaneous knock down of Rassf5 and induction of Hras^{G12V} expression. **(D)** Quantification of differentiation using EdU-BrdU pulse/chase differentiation assay. Depletion of Rassf5 promotes renewal in Hras^{G12V} epidermis. **(E)** Diagram of construct containing Rassf5 ORF fused with tdTomato (Rassf5-tdT) and co-expressing Cre. **(F)** Representative images of Hras^{G12V} clone and Hras^{G12V}; Rassf5-tdT clone in E18.5 epidermis. Overexpression of Rassf5 yields clones with reduced basal and extensive suprabasal compartment. Scale bar is 25 µm. **(G)** Whole mount images of Hras^{G12V} clone and Hras^{G12V}; Rassf5-tdT clone in E18.5 epidermis. Scale bar is 25µm. **(H)** Quantification of basal cell

numbers in E18.5 $Hras^{G12V}$ and $Hras^{G12V}$;Rassf5-tdT clones. **(I)** Quantification of the ratio of suprabasal surface area to basal surface area of $Hras^{G12V}$ and $Hras^{G12V}$; Rassf5-tdT clones in E18.5 epidermis. For **H,I** each dot represents an individual clone. For **A,D,H,I** statistics were based on n≧3 animals for each condition; the center line represents the mean and errors bars the s.d. Two-tailed Student's t-tests were used. n.s. denotes p value >0.05. * denotes p value <0.05; ** denotes p value <0.01*** denotes p value <0.001.

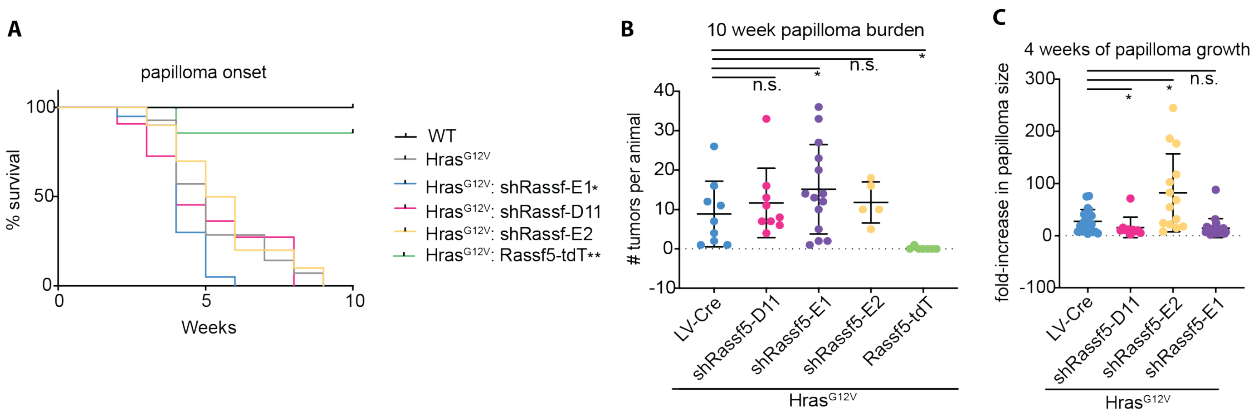

Figure 11 Rassf5 overexpression prevents papilloma formation in $Hras^{G12V}$ animals. **(A)** Kaplan-Meier survival plot of $Hras^{G12V}$, $Hras^{G12V}$; shRassf5, and $Hras^{G12V}$; Rassf5-tdT mice. **(B)** Quantification of papillomas per animal in $Hras^{G12V}$, $Hras^{G12V}$; shRassf5, and $Hras^{G12V}$. Transduction rate was not considered during calculations. **(C)** Normalized papilloma growth in $Hras^{G12V}$ and $Hras^{G12V}$; shRassf5 animals.

Chapter 6—Discussion

6.1 The merits of cell fate identification assay

Previous studies have utilized spindle orientation to determine apical or basal division in developing epidermis (Luxenburg et al., 2011; Williams et al., 2014). This assay assumes if the mitotic spindle is oriented parallel to the basement membrane, the resulting division will produce two daughter cells that maintain the progenitor potential of the mother cell. Conversely, if the mitotic spindle is oriented perpendicular to the membrane, this would result in the apical daughter cell differentiating and the basal daughter remaining a progenitor. Though this technique has established that stratification during development correlates with an increase in the number of divisions oriented perpendicular to the basement membrane, it assumes ultimate cell fate choices and precludes symmetric differentiation entirely, an event which we and others have shown is common in adult epidermis (Rompolas et al., 2016; Ying et al., 2018) . In contrast to the oriented divisions seen in developing epidermis, intra-vital imaging has demonstrated that adult epidermal progenitor cells exclusively divide in plane with the basement membrane and then move according to differentiation state. Though decidedly useful in studying the epidermis, intra-vital imaging is highly technical and cost prohibitive.

To rectify the limitations of these current methods, we developed a novel cell fate identification (CFI) assay, which is characterized by several features, which should make it a standard in the field:

(i) it quantifies progenitor renewal and differentiation rates *in vivo*—by including net effects of direct and indirect determinants such as spindle orientation, delamination and plasticity, it reports the ultimate daughter cell fate choice;

(ii) it records progenitor/daughter cell locations—by maintaining spatial information of progenitor fate decisions, it allows for analysis of heterogeneity that may be driven by specific cell/cell and cell/niche interactions;

(iii) it is an approachable assay—by utilizing generic reagents and microscopy techniques, it is easily assimilated into any research program.

This assay allowed us to quantify progenitor renewal and proliferation rates in the context of cell location, enabling us to study oncogene growth inhibition in the epidermis.

6.2 Potential Rassf5 pro-differentiation mechanisms

Using CFI we quantified the changes in progenitor fate choices in oncogenic clones. The dynamic renewal/differentiation rates lead us to conduct a genetic screen of Ras effectors to understand the mechanism behind our finding. We have identified a specific Ras effector, Rassf5, as a critical regulator of differentiation. Rassf5 has been shown to interact with the Hippo pathway. Hippo signaling is important during development and is critical in regulating organ size (Justice et al., 1995; Tapon et al., 2002). Hippo was first thought to be relevant to cancer when researchers discovered that it restricted the growth of *Drosophila* tissues. Over the years, additional evidence pointed to Hippo signaling being dysregulated in cancer, with certain Hippo gene mutations causing tumors. The canonical Hippo pathway involves kinases Mst1/2 (homologues of *Drosophila* Hippo) and Sav1 complexing with Lats1/2, which then phosphorylates Yap. This phosphorylation causes Yap to be degraded (Figure 12). When not phosphorylated, Yap

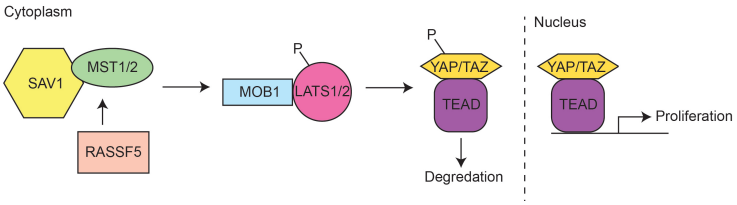

Figure 12: The Hippo pathway leads to the phosphorylation and subsequent degradation of YAP/TAZ. When YAP/TAZ is not phosphorylated, it can enter the nucleus and activate transcription of pro-proliferation target genes. Adapted from (Pfeifer et al., 2010)

translocates to the nucleus and promotes viability and tissue growth by controlling the actions of several transcription factors including Tead and Smad (Harvey et al., 2013).

Rassf5 and other family members have an effect on the Hippo pathway. Rassf1, Rassf5, and Rassf6 binds to Mst1 or Mst2 thereby mediating apoptosis or affecting cell cycle length (Aoyama et al., 2004; Guo et al., 2007; Ikeda et al., 2009). Rassf5 is able to complex with Mst1/2 via its SARAH domain (Bitra et al., 2017). Mst1 can induce apoptosis via phosphorylation of histone H2B (Cheung et al., 2003; Ura et al., 2001). Because Rassf5 interaction with Mst1 allows it to more readily phosphorylate histone H2B, it is thought that the Rassf5/Mst1 interaction is pro-apoptotic (Bitra et al., 2017). Here, we hypothesize that the binding of Ras with Rassf5/Mst1 could activate Mst1 and promote phosphorylation of Lats1/2, which leads to degradation of Yap. Previous study of Yap in murine epidermis has shown that it is expressed almost exclusively in the basal layer and promotes progenitor maintenance (Zhang et al., 2011). This observation correlates with our hypothesis of Rassf5 interaction with the Hippo pathway. If Rassf5 activation of Mst1 eventually leads to the degradation of Yap, this would cause cells to lose progenitor identity and instead differentiate.

Though Rassf5 has not been connected with differentiation in keratinocytes before now, another study linked Rassf5 to *trans*-retinoic acid-induced differentiation in a MYCN amplified neuroblastoma cell line (Das et al., 2010). The retinoic acid pathway is vital during development and is important in the differentiation processes of many cells, including neurons (Bibel et al., 2004; Rhinn and Dollé, 2012). Retinoic acid signaling in the epidermis is complex. For decades, retinoic acid has been used clinically as an anti-aging therapy and for treatment of acne vulgaris (Leyden et al., 2014). Topical retinoic acid application causes the skin to thicken as the keratinocytes stratify and differentiate, generating hyperplasia. Animals expressing a dominant

negative retinoic acid receptor (RAR), which inhibits retinoic acid signaling, developed thin skin which lacked hair follicles, and keratinocyte differentiation markers were also aberrantly expressed. Furthermore, the K5-expressing basal cell population expanded and there was less keratin expression overall, leading the authors to conclude that inhibiting retinoic acid signaling lead to an immature epidermis (Saitou et al., 1995) Further study indicated that the retinoic acid pathway is not important during epidermal homeostasis because it does not take part in promoting the renewal of keratinocytes in adult animals (Chapellier et al., 2002). Though the precise mechanism of RAR signalizing in epidermis is unknown, we can conclude that RAR signaling contributes to epidermis development and alters keratinocyte differentiation processes. In the context of this study, we propose that Rassf5 could promote differentiation by activating RAR signaling. Further study of Rassf5's pro-differentiation activities and a possible link to the RAR signaling pathway would be interesting.

6.3 Implications of oncogenic clone heterogeneity in cell fate choices and cell competition

The idea of differentiation as a method to stall oncogenic growth has gained traction in recent years (Brown et al., 2017; Ying et al., 2018). Originally, the primary methods of preventing oncogene-driven clonal expansion in the epidermis were thought to be through senescence and apoptosis, with senescence in particular acting as a blockade to tumor growth (Braig et al., 2005; Fearnhead et al., 1998; Michaloglou et al., 2005). These processes, however, both limit tissue proliferation and eventually disrupt epithelial function. Furthermore, observations that phenotypically normal skin contains a large number of clones under positive selection contradicts the idea of apoptosis or senescence playing a large role in preventing clonal expansion (Martincorena et al., 2018; Martincorena et al., 2015).

Because renewal and differentiation are a natural part of epidermal maintenance, it follows that the tissue would rely on this mechanism to inhibit aberrant growth. A study of developing mouse embryos revealed that less fit $Mycn^{+/-}$ cells undergo apoptosis more often when adjacent to a WT cell. During the later stages of gestation, when apoptosis is not common in the epidermis, these $Mycn^{+/-}$ clones underwent more differentiating divisions, eventually leading to clone loss (Ellis et al., 2019). This suggests that differentiation as a method of rectifying damaged cells is a naturally occurring part of epidermal function.

Our work contributes to this field by demonstrating that the growth of a single, isolated oncogenic clone can be stalled through the interplay of renewing and differentiating events within the clone. This action illuminates how clones driven by potent mutations grew to limited and relatively uniform sizes in aged epidermis (Martincorena et al., 2015). Together, these data indicate that the skin uses differentiation as its primary growth-suppressive mechanism.

The precise manipulation of progenitor fate choices in distinct compartments of oncogenic clones raises questions about how epidermal basal cells specifically assign fate choice. In the fly, oriented divisions allow stem cells to either remain in the niche and maintain stemness or leave the niche and differentiate. In contrast to this, basal cells of the adult epidermis divide in plane with the basement membrane and then move according to their fate. This action suggests asymmetric inheritance of renewal/differentiation drivers, since both daughter cells remain in the progenitor environment and are still in contact with renewal factors such as integrins. Numb can be asymmetrically inherited in keratinocytes (Clayton et al., 2007), allowing the possibility for other factors to be distributed preferentially to each daughter cell.

Dividing in plane with the basement membrane may also provide a means to initiate differentiation as needed by the local environment. If differentiation was predetermined,

progenitors would be committed to a specific fate and could not adapt to local conditions. Basal cells are thought to divide stochastically, with daughter cells choosing their differentiation state as required to maintain homeostasis (Clayton et al., 2007; Mesa et al., 2018). This mechanism provides a ready response to address local needs and maintain homeostasis.

The possibility that cell fate is linked to local conditions gives insight into the influence of the heterotypic environment on cell fate choices of $Hras^{G12V}$ clones. WT cells can sense and respond to mutant cells (Brown et al., 2017; Hogan et al., 2009; Watanabe et al., 2018), generating the possibility that WT cells initiate the change in $Hras^{G12V}$ clone renewal. However, it seems unlikely that WT cells would be directly causing an impact on $Hras^{G12V}$ renewal rate because the renewal rate of edge cells in late stage clones is very similar to that of $Hras^{G12V}$ single cells. What is more striking is the reason behind the pro-differentiation fate choices of the inner cells, which suggests that interaction between neighboring $Hras^{G12V}$ cells is detrimental to their long-term survival. How the differentiation of the inner cell is initiated is unknown but would be an intriguing avenue of further study.

Changes in cell behavior because of heterotypic adhesions have been well documented (Mishra et al., 2019). The migration of *Drosophila* border cells and polar cells during ovary development is dependent on E-cadherin connecting the two cell types (Montell, 2003). In mammals, heterotypic adhesions are seen in the terminal end bud where neogenin-netrin interactions connect migratory luminal cells and cap cells. If either neogenin or netrin are not expressed, then the structure disassociates (Srinivasan et al., 2003). These observations have implications for this study. The dynamic behavior that we observe in $Hras^{G12V}$ clones could be due in part to the homotypic or heterotypic environments of dividing cells. In $Hras^{G12V}$ clones, the homogeneous environment of the inner core resulted in pro-differentiation daughter cells. It is

plausible that the homotypic adhesions of $Hras^{G12V}$/$Hras^{G12V}$ inner cells could promote recruitment of more Ras and/or more Rassf5 to the membrane, driving an increase in differentiation. Additional work from our lab identifies increased Eif2b5-dependent translation of Rassf5 in $Hras^{G12V}$ animals (Cai, 2019) suggesting that homotypic $Hras^{G12V}$ neighbors may have higher rates of translation, driving Rassf5 expression.

The pro-differentiation nature of the core $Hras^{G12V}$ cells has implications in cell competition, a process that is known to occur in the epidermis. During development, less fit clones are removed via differentiation (Ellis et al., 2019). In the adult animal, epidermal clones associated with high expression of the hemidesmosome Col17A1 are more fit and out compete clones associated with low levels of Col17A1. Researchers hypothesized that Col17A1 promoted renewal in basal cells, which increased the longevity of the clone (Liu et al., 2019). In terms of this study, the "more-fit" edge cells of the $Hras^{G12V}$ clone could be inducing the differentiation of the "less-fit" inner cells. The balance between the fates of these two populations leads to a near-homeostatic renewal rate of the entire clone.

My work over the last five years demonstrates that a slight change in renewal rate can alter the expansion of a clone dramatically, indicating that dynamic control of renewal rates is an efficient method of stalling oncogenic growth and effectively decreasing clone fitness. $Hras^{G12V}$ cells divide more rapidly than WT cells yet decreasing renewal alone can inhibit growth, further indicating the strength of renewal/differentiation interplay in impeding a clone's progress and maintaining tissue integrity. We conclude that epidermis not only limits the growth of a multitude of clones but also can do so on a single clone basis.

References

Adams, J.C., and Watt, F.M. (1989). Fibronectin inhibits the terminal differentiation of human keratinocytes. Nature *340*, 307-309.

Aoyama, Y., Avruch, J., and Zhang, X.F. (2004). Nore1 inhibits tumor cell growth independent of Ras or the MST1/2 kinases. Oncogene *23*, 3426-3433.

Balmain, A., and Pragnell, I.B. (1983). Mouse skin carcinomas induced in vivo by chemical carcinogens have a transforming Harvey-ras oncogene. Nature *303*, 72-74.

Beronja, S., and Fuchs, E. (2013). RNAi-mediated gene function analysis in skin. Methods Mol Biol *961*, 351-361.

Beronja, S., Janki, P., Heller, E., Lien, W.H., Keyes, B.E., Oshimori, N., and Fuchs, E. (2013). RNAi screens in mice identify physiological regulators of oncogenic growth. Nature *501*, 185-190.

Beronja, S., Livshits, G., Williams, S., and Fuchs, E. (2010). Rapid functional dissection of genetic networks via tissue-specific transduction and RNAi in mouse embryos. Nat Med *16*, 821-827.

Bibel, M., Richter, J., Schrenk, K., Tucker, K.L., Staiger, V., Korte, M., Goetz, M., and Barde, Y.A. (2004). Differentiation of mouse embryonic stem cells into a defined neuronal lineage. Nat Neurosci *7*, 1003-1009.

Bitra, A., Sistla, S., Mariam, J., Malvi, H., and Anand, R. (2017). Rassf Proteins as Modulators of Mst1 Kinase Activity. Sci Rep *7*, 45020.

Blau, H.M., and Baltimore, D. (1991). Differentiation requires continuous regulation. J Cell Biol *112*, 781-783.

Bowling, S., Lawlor, K., and Rodriguez, T.A. (2019). Cell competition: the winners and losers of fitness selection. Development *146*.

Braig, M., Lee, S., Loddenkemper, C., Rudolph, C., Peters, A.H., Schlegelberger, B., Stein, H., Dorken, B., Jenuwein, T., and Schmitt, C.A. (2005). Oncogene-induced senescence as an initial barrier in lymphoma development. Nature *436*, 660-665.

Brown, S., Pineda, C.M., Xin, T., Boucher, J., Suozzi, K.C., Park, S., Matte-Martone, C., Gonzalez, D.G., Rytlewski, J., Beronja, S.*, et al.* (2017). Correction of aberrant growth preserves tissue homeostasis. Nature *548*, 334-337.

Cai, Y. (2019). Translational mechanisms of stem cell fate regulation in epidermal oncogene tolerance. In Molecular and Cellular Biology (University of Washington).

Castellano, E., Sheridan, C., Thin, M.Z., Nye, E., Spencer-Dene, B., Diefenbacher, M.E., Moore, C., Kumar, M.S., Murillo, M.M., Gronroos, E.*, et al.* (2013). Requirement for interaction of PI3-kinase p110alpha with RAS in lung tumor maintenance. Cancer Cell *24*, 617-630.

Chapellier, B., Mark, M., Messaddeq, N., Calleja, C., Warot, X., Brocard, J., Gerard, C., Li, M., Metzger, D., Ghyselinck, N.B.*, et al.* (2002). Physiological and retinoid-induced proliferations of epidermis basal keratinocytes are differently controlled. Embo j *21*, 3402-3413.

Chen, X., Mitsutake, N., LaPerle, K., Akeno, N., Zanzonico, P., Longo, V.A., Mitsutake, S., Kimura, E.T., Geiger, H., Santos, E.*, et al.* (2009). Endogenous expression of Hras(G12V) induces developmental defects and neoplasms with copy number imbalances of the oncogene. Proc Natl Acad Sci U S A *106*, 7979-7984.

Cheung, W.L., Ajiro, K., Samejima, K., Kloc, M., Cheung, P., Mizzen, C.A., Beeser, A., Etkin, L.D., Chernoff, J., Earnshaw, W.C.*, et al.* (2003). Apoptotic phosphorylation of histone H2B is mediated by mammalian sterile twenty kinase. Cell *113*, 507-517.

Clayton, E., Doupe, D.P., Klein, A.M., Winton, D.J., Simons, B.D., and Jones, P.H. (2007). A single type of progenitor cell maintains normal epidermis. Nature *446*, 185-189.

Coulombre, J.L., and Coulombre, A.J. (1971). Metaplastic induction of scales and feathers in the corneal anterior epithelium of the chick embryo. Dev Biol *25*, 464-478.

Dajee, M., Tarutani, M., Deng, H., Cai, T., and Khavari, P.A. (2002). Epidermal Ras blockade demonstrates spatially localized Ras promotion of proliferation and inhibition of differentiation. Oncogene *21*, 1527-1538.

Das, S., Foley, N., Bryan, K., Watters, K.M., Bray, I., Murphy, D.M., Buckley, P.G., and Stallings, R.L. (2010). MicroRNA mediates DNA demethylation events triggered by retinoic acid during neuroblastoma cell differentiation. Cancer Res *70*, 7874-7881.

de la Cova, C., Abril, M., Bellosta, P., Gallant, P., and Johnston, L.A. (2004). Drosophila myc regulates organ size by inducing cell competition. Cell *117*, 107-116.

DeCosse, J.J., Gossens, C.L., Kuzma, J.F., and Unsworth, B.R. (1973). Breast cancer: induction of differentiation by embryonic tissue. Science *181*, 1057-1058.

Donninger, H., Calvisi, D.F., Barnoud, T., Clark, J., Schmidt, M.L., Vos, M.D., and Clark, G.J. (2015). NORE1A is a Ras senescence effector that controls the apoptotic/senescent balance of p53 via HIPK2. J Cell Biol *208*, 777-789.

Donninger, H., Schmidt, M.L., Mezzanotte, J., Barnoud, T., and Clark, G.J. (2016). Ras signaling through RASSF proteins. Semin Cell Dev Biol *58*, 86-95.

Dotto, G.P., and Rustgi, A.K. (2016). Squamous Cell Cancers: A Unified Perspective on Biology and Genetics. Cancer Cell *29*, 622-637.

Doupe, D.P., Klein, A.M., Simons, B.D., and Jones, P.H. (2010). The ordered architecture of murine ear epidermis is maintained by progenitor cells with random fate. Dev Cell *18*, 317-323.

Downward, J. (2003). Targeting RAS signalling pathways in cancer therapy. Nat Rev Cancer *3*, 11-22.

Eisenhoffer, G.T., Loftus, P.D., Yoshigi, M., Otsuna, H., Chien, C.B., Morcos, P.A., and Rosenblatt, J. (2012). Crowding induces live cell extrusion to maintain homeostatic cell numbers in epithelia. Nature *484*, 546-549.

Ellis, S.J., Gomez, N.C., Levorse, J., Mertz, A.F., Ge, Y., and Fuchs, E. (2019). Distinct modes of cell competition shape mammalian tissue morphogenesis. Nature *569*, 497-502.

Elmetwali, T., Salman, A., and Palmer, D.H. (2016). NORE1A induction by membrane-bound CD40L (mCD40L) contributes to CD40L-induced cell death and G1 growth arrest in p21-mediated mechanism. Cell Death Dis *7*, e2146.

Fearnhead, H.O., Rodriguez, J., Govek, E.E., Guo, W., Kobayashi, R., Hannon, G., and Lazebnik, Y.A. (1998). Oncogene-dependent apoptosis is mediated by caspase-9. Proc Natl Acad Sci U S A *95*, 13664-13669.

Fernandez-Medarde, A., and Santos, E. (2011). Ras in cancer and developmental diseases. Genes Cancer *2*, 344-358.

Fujiwara, H., Ferreira, M., Donati, G., Marciano, D.K., Linton, J.M., Sato, Y., Hartner, A., Sekiguchi, K., Reichardt, L.F., and Watt, F.M. (2011). The basement membrane of hair follicle stem cells is a muscle cell niche. Cell *144*, 577-589.

Goldstein, B., and Macara, I.G. (2007). The PAR proteins: fundamental players in animal cell polarization. Dev Cell *13*, 609-622.

Gonzales, K.A.U., and Fuchs, E. (2017). Skin and Its Regenerative Powers: An Alliance between Stem Cells and Their Niche. Dev Cell *43*, 387-401.

Guo, C., Tommasi, S., Liu, L., Yee, J.K., Dammann, R., and Pfeifer, G.P. (2007). RASSF1A is part of a complex similar to the Drosophila Hippo/Salvador/Lats tumor-suppressor network. Curr Biol *17*, 700-705.

Guo, W., Wang, C., Guo, Y., Shen, S., Guo, X., Kuang, G., and Dong, Z. (2015). RASSF5A, a candidate tumor suppressor, is epigenetically inactivated in esophageal squamous cell carcinoma. Clin Exp Metastasis *32*, 83-98.

Gupta, S., Ramjaun, A.R., Haiko, P., Wang, Y., Warne, P.H., Nicke, B., Nye, E., Stamp, G., Alitalo, K., and Downward, J. (2007). Binding of ras to phosphoinositide 3-kinase p110alpha is required for ras-driven tumorigenesis in mice. Cell *129*, 957-968.

Harvey, K.F., Zhang, X., and Thomas, D.M. (2013). The Hippo pathway and human cancer. Nat Rev Cancer *13*, 246-257.

Higa, K.C., and DeGregori, J. (2019). Decoy fitness peaks, tumor suppression, and aging. Aging Cell *18*, e12938.

Hogan, C., Dupre-Crochet, S., Norman, M., Kajita, M., Zimmermann, C., Pelling, A.E., Piddini, E., Baena-Lopez, L.A., Vincent, J.P., Itoh, Y.*, et al.* (2009). Characterization of the interface between normal and transformed epithelial cells. Nat Cell Biol *11*, 460-467.

Ikeda, M., Kawata, A., Nishikawa, M., Tateishi, Y., Yamaguchi, M., Nakagawa, K., Hirabayashi, S., Bao, Y., Hidaka, S., Hirata, Y.*, et al.* (2009). Hippo pathway-dependent and -independent roles of RASSF6. Sci Signal *2*, ra59.

Ito, M., Liu, Y., Yang, Z., Nguyen, J., Liang, F., Morris, R.J., and Cotsarelis, G. (2005). Stem cells in the hair follicle bulge contribute to wound repair but not to homeostasis of the epidermis. Nat Med *11*, 1351-1354.

Justice, R.W., Zilian, O., Woods, D.F., Noll, M., and Bryant, P.J. (1995). The Drosophila tumor suppressor gene warts encodes a homolog of human myotonic dystrophy kinase and is required for the control of cell shape and proliferation. Genes Dev *9*, 534-546.

Karnoub, A.E., and Weinberg, R.A. (2008). Ras oncogenes: split personalities. Nat Rev Mol Cell Biol *9*, 517-531.

Knoblich, J.A. (2008). Mechanisms of asymmetric stem cell division. Cell *132*, 583-597.

Le Borgne, R., Bardin, A., and Schweisguth, F. (2005). The roles of receptor and ligand endocytosis in regulating Notch signaling. Development *132*, 1751-1762.

Lechler, T., and Fuchs, E. (2007). Desmoplakin: an unexpected regulator of microtubule organization in the epidermis. J Cell Biol *176*, 147-154.

Lee, Y.S., Yuspa, S.H., and Dlugosz, A.A. (1998). Differentiation of cultured human epidermal keratinocytes at high cell densities is mediated by endogenous activation of the protein kinase C signaling pathway. J Invest Dermatol *111*, 762-766.

Levy, V., Lindon, C., Harfe, B.D., and Morgan, B.A. (2005). Distinct stem cell populations regenerate the follicle and interfollicular epidermis. Dev Cell *9*, 855-861.

Leyden, J.J., Del Rosso, J.Q., and Baum, E.W. (2014). The use of isotretinoin in the treatment of acne vulgaris: clinical considerations and future directions. J Clin Aesthet Dermatol *7*, S3-s21.

Lindner, G., Botchkarev, V.A., Botchkareva, N.V., Ling, G., van der Veen, C., and Paus, R. (1997). Analysis of apoptosis during hair follicle regression (catagen). Am J Pathol *151*, 1601-1617.

Liu, N., Matsumura, H., Kato, T., Ichinose, S., Takada, A., Namiki, T., Asakawa, K., Morinaga, H., Mohri, Y., De Arcangelis, A.*, et al.* (2019). Stem cell competition orchestrates skin homeostasis and ageing. Nature *568*, 344-350.

Love, M.I., Huber, W., and Anders, S. (2014). Moderated estimation of fold change and dispersion for RNA-seq data with DESeq2. Genome Biology *15*, 550.

Luxenburg, C., Pasolli, H.A., Williams, S.E., and Fuchs, E. (2011). Developmental roles for Srf, cortical cytoskeleton and cell shape in epidermal spindle orientation. Nat Cell Biol *13*, 203-214.

Martincorena, I., Fowler, J.C., Wabik, A., Lawson, A.R.J., Abascal, F., Hall, M.W.J., Cagan, A., Murai, K., Mahbubani, K., Stratton, M.R.*, et al.* (2018). Somatic mutant clones colonize the human esophagus with age. Science *362*, 911-917.

Martincorena, I., Roshan, A., Gerstung, M., Ellis, P., Van Loo, P., McLaren, S., Wedge, D.C., Fullam, A., Alexandrov, L.B., Tubio, J.M.*, et al.* (2015). Tumor evolution. High burden and pervasive positive selection of somatic mutations in normal human skin. Science *348*, 880-886.

Mascre, G., Dekoninck, S., Drogat, B., Youssef, K.K., Brohee, S., Sotiropoulou, P.A., Simons, B.D., and Blanpain, C. (2012). Distinct contribution of stem and progenitor cells to epidermal maintenance. Nature *489*, 257-262.

Mecklenburg, L., Tobin, D.J., Muller-Rover, S., Handjiski, B., Wendt, G., Peters, E.M., Pohl, S., Moll, I., and Paus, R. (2000). Active hair growth (anagen) is associated with angiogenesis. J Invest Dermatol *114*, 909-916.

Mesa, K.R., Kawaguchi, K., Cockburn, K., Gonzalez, D., Boucher, J., Xin, T., Klein, A.M., and Greco, V. (2018). Homeostatic Epidermal Stem Cell Self-Renewal Is Driven by Local Differentiation. Cell Stem Cell *23*, 677-686.e674.

Michaloglou, C., Vredeveld, L.C., Soengas, M.S., Denoyelle, C., Kuilman, T., van der Horst, C.M., Majoor, D.M., Shay, J.W., Mooi, W.J., and Peeper, D.S. (2005). BRAFE600-associated senescence-like cell cycle arrest of human naevi. Nature *436*, 720-724.

Mintz, B., and Illmensee, K. (1975). Normal genetically mosaic mice produced from malignant teratocarcinoma cells. Proc Natl Acad Sci U S A *72*, 3585-3589.

Mishra, A.K., Campanale, J.P., Mondo, J.A., and Montell, D.J. (2019). Cell interactions in collective cell migration. Development *146*.

Montell, D.J. (2003). Border-cell migration: the race is on. Nat Rev Mol Cell Biol *4*, 13-24.

Morata, G., and Ripoll, P. (1975). Minutes: mutants of drosophila autonomously affecting cell division rate. Dev Biol *42*, 211-221.

Moreno, E., and Basler, K. (2004). dMyc transforms cells into super-competitors. Cell *117*, 117-129.

Morris, R.J., Liu, Y., Marles, L., Yang, Z., Trempus, C., Li, S., Lin, J.S., Sawicki, J.A., and Cotsarelis, G. (2004). Capturing and profiling adult hair follicle stem cells. Nat Biotechnol *22*, 411-417.

Murai, K., Skrupskelyte, G., Piedrafita, G., Hall, M., Kostiou, V., Ong, S.H., Nagy, T., Cagan, A., Goulding, D., Klein, A.M*., et al.* (2018). Epidermal Tissue Adapts to Restrain Progenitors Carrying Clonal p53 Mutations. Cell Stem Cell *23*, 687-699 e688.

Muzumdar, M.D., Tasic, B., Miyamichi, K., Li, L., and Luo, L. (2007). A global double-fluorescent Cre reporter mouse. Genesis *45*, 593-605.

Myung, P., and Ito, M. (2012). Dissecting the bulge in hair regeneration. J Clin Invest *122*, 448-454.

Nelson, C.M., and Bissell, M.J. (2006). Of extracellular matrix, scaffolds, and signaling: tissue architecture regulates development, homeostasis, and cancer. Annu Rev Cell Dev Biol *22*, 287-309.

Nikolopoulos, S.N., Blaikie, P., Yoshioka, T., Guo, W., Puri, C., Tacchetti, C., and Giancotti, F.G. (2005). Targeted deletion of the integrin beta4 signaling domain suppresses laminin-5-dependent nuclear entry of mitogen-activated protein kinases and NF-kappaB, causing defects in epidermal growth and migration. Mol Cell Biol *25*, 6090-6102.

Oliver, E.R., Saunders, T.L., Tarlé, S.A., and Glaser, T. (2004). Ribosomal protein L24 defect in Belly spot and tail (Bst), a mouse Minute. Development *131*, 3907-3920.

Oshima, H., Rochat, A., Kedzia, C., Kobayashi, K., and Barrandon, Y. (2001). Morphogenesis and renewal of hair follicles from adult multipotent stem cells. Cell *104*, 233-245.

Park, J., Kang, S.I., Lee, S.Y., Zhang, X.F., Kim, M.S., Beers, L.F., Lim, D.S., Avruch, J., Kim, H.S., and Lee, S.B. (2010). Tumor suppressor ras association domain family 5 (RASSF5/NORE1) mediates death receptor ligand-induced apoptosis. J Biol Chem *285*, 35029-35038.

Parsa, R., Yang, A., McKeon, F., and Green, H. (1999). Association of p63 with proliferative potential in normal and neoplastic human keratinocytes. J Invest Dermatol *113*, 1099-1105.

Pfeifer, G.P., Dammann, R., and Tommasi, S. (2010). RASSF proteins. Curr Biol *20*, R344-345.

Poumay, Y., and Pittelkow, M.R. (1995). Cell density and culture factors regulate keratinocyte commitment to differentiation and expression of suprabasal K1/K10 keratins. J Invest Dermatol *104*, 271-276.

Quintanilla, M., Brown, K., Ramsden, M., and Balmain, A. (1986). Carcinogen-specific mutation and amplification of Ha-ras during mouse skin carcinogenesis. Nature *322*, 78-80.

Rhinn, M., and Dollé, P. (2012). Retinoic acid signalling during development. Development *139*, 843-858.

Rochat, A., Kobayashi, K., and Barrandon, Y. (1994). Location of stem cells of human hair follicles by clonal analysis. Cell *76*, 1063-1073.

Rompolas, P., Deschene, E.R., Zito, G., Gonzalez, D.G., Saotome, I., Haberman, A.M., and Greco, V. (2012). Live imaging of stem cell and progeny behaviour in physiological hair-follicle regeneration. Nature *487*, 496-499.

Rompolas, P., Mesa, K.R., and Greco, V. (2013). Spatial organization within a niche as a determinant of stem-cell fate. Nature *502*, 513-518.

Rompolas, P., Mesa, K.R., Kawaguchi, K., Park, S., Gonzalez, D., Brown, S., Boucher, J., Klein, A.M., and Greco, V. (2016). Spatiotemporal coordination of stem cell commitment during epidermal homeostasis. Science *352*, 1471-1474.

Sada, A., Jacob, F., Leung, E., Wang, S., White, B.S., Shalloway, D., and Tumbar, T. (2016). Defining the cellular lineage hierarchy in the interfollicular epidermis of adult skin. Nat Cell Biol *18*, 619-631.

Saitou, M., Sugai, S., Tanaka, T., Shimouchi, K., Fuchs, E., Narumiya, S., and Kakizuka, A. (1995). Inhibition of skin development by targeted expression of a dominant-negative retinoic acid receptor. Nature *374*, 159-162.

Sakakura, T., Nishizuka, Y., and Dawe, C.J. (1976). Mesenchyme-dependent morphogenesis and epithelium-specific cytodifferentiation in mouse mammary gland. Science *194*, 1439-1441.

Scheffzek, K., Ahmadian, M.R., Kabsch, W., Wiesmuller, L., Lautwein, A., Schmitz, F., and Wittinghofer, A. (1997). The Ras-RasGAP complex: structural basis for GTPase activation and its loss in oncogenic Ras mutants. Science *277*, 333-338.

Schweisguth, F. (2004). Regulation of notch signaling activity. Curr Biol *14*, R129-138.

Sotiropoulou, P.A., and Blanpain, C. (2012). Development and homeostasis of the skin epidermis. Cold Spring Harb Perspect Biol *4*, a008383.

Srinivasan, K., Strickland, P., Valdes, A., Shin, G.C., and Hinck, L. (2003). Netrin-1/neogenin interaction stabilizes multipotent progenitor cap cells during mammary gland morphogenesis. Dev Cell *4*, 371-382.

Steinmann, K., Sandner, A., Schagdarsurengin, U., and Dammann, R.H. (2009). Frequent promoter hypermethylation of tumor-related genes in head and neck squamous cell carcinoma. Oncol Rep *22*, 1519-1526.

Suzuki, A., and Ohno, S. (2006). The PAR-aPKC system: lessons in polarity. J Cell Sci *119*, 979-987.

Tapon, N., Harvey, K.F., Bell, D.W., Wahrer, D.C., Schiripo, T.A., Haber, D., and Hariharan, I.K. (2002). salvador Promotes both cell cycle exit and apoptosis in Drosophila and is mutated in human cancer cell lines. Cell *110*, 467-478.

Tomasetti, C., and Levy, D. (2010). Role of symmetric and asymmetric division of stem cells in developing drug resistance. Proc Natl Acad Sci U S A *107*, 16766-16771.

Tomayko, M.M., and Reynolds, C.P. (1989). Determination of subcutaneous tumor size in athymic (nude) mice. Cancer Chemother Pharmacol *24*, 148-154.

Tumbar, T., Guasch, G., Greco, V., Blanpain, C., Lowry, W.E., Rendl, M., and Fuchs, E. (2004). Defining the epithelial stem cell niche in skin. Science *303*, 359-363.

Ura, S., Masuyama, N., Graves, J.D., and Gotoh, Y. (2001). MST1-JNK promotes apoptosis via caspase-dependent and independent pathways. Genes Cells *6*, 519-530.

Vasioukhin, V., Degenstein, L., Wise, B., and Fuchs, E. (1999). The magical touch: genome targeting in epidermal stem cells induced by tamoxifen application to mouse skin. Proc Natl Acad Sci U S A *96*, 8551-8556.

Vavvas, D., Li, X., Avruch, J., and Zhang, X.F. (1998). Identification of Nore1 as a potential Ras effector. J Biol Chem *273*, 5439-5442.

Watanabe, H., Ishibashi, K., Mano, H., Kitamoto, S., Sato, N., Hoshiba, K., Kato, M., Matsuzawa, F., Takeuchi, Y., Shirai, T.*, et al.* (2018). Mutant p53-Expressing Cells Undergo Necroptosis via Cell Competition with the Neighboring Normal Epithelial Cells. Cell Rep *23*, 3721-3729.

Watt, F.M., and Jones, P.H. (1993). Expression and function of the keratinocyte integrins. Dev Suppl, 185-192.

Williams, S.E., Beronja, S., Pasolli, H.A., and Fuchs, E. (2011). Asymmetric cell divisions promote Notch-dependent epidermal differentiation. Nature *470*, 353-358.

Williams, S.E., Ratliff, L.A., Postiglione, M.P., Knoblich, J.A., and Fuchs, E. (2014). Par3-mInsc and Galphai3 cooperate to promote oriented epidermal cell divisions through LGN. Nat Cell Biol *16*, 758-769.

Yang, A., Kaghad, M., Wang, Y., Gillett, E., Fleming, M.D., Dotsch, V., Andrews, N.C., Caput, D., and McKeon, F. (1998). p63, a p53 homolog at 3q27-29, encodes multiple products with transactivating, death-inducing, and dominant-negative activities. Mol Cell *2*, 305-316.

Yang, A., Schweitzer, R., Sun, D., Kaghad, M., Walker, N., Bronson, R.T., Tabin, C., Sharpe, A., Caput, D., Crum, C.*, et al.* (1999). p63 is essential for regenerative proliferation in limb, craniofacial and epithelial development. Nature *398*, 714-718.

Ying, Z., Sandoval, M., and Beronja, S. (2018). Oncogenic activation of PI3K induces progenitor cell differentiation to suppress epidermal growth. Nat Cell Biol *20*, 1256-1266.

Zhang, H., Pasolli, H.A., and Fuchs, E. (2011). Yes-associated protein (YAP) transcriptional coactivator functions in balancing growth and differentiation in skin. Proc Natl Acad Sci U S A *108*, 2270-2275.